LAWRENCE
LIVERMORE
NATIONAL
LABORATORY

LLNL-JRNL-493852

Understanding Differences in Current Cloud Retrievals of ARM Ground-based Measurements

C. Zhao, S. Xie, S. A. Klein, A. Protat, M. D. Shupe, S. A. McFarlane, J. M. Comstock, J. Delanoe, M. Deng, M. Dunn, R. J. Hogan, D. Huang, M. P. Jensen, G. G. Mace, R. McCoy, E. J. O'Connor, D. Turner, Z. Wang

August 17, 2011

Journal of Geophysical Research-Atmosphere

Disclaimer

Toward Understanding of Differences in Current Cloud Retrievals of ARM Ground-based Measurements

Chuanfeng Zhao[1*], Shaocheng Xie[1], Stephen A. Klein[1], Alain Protat[2,3], Matthew D. Shupe[4], Sally A. McFarlane[5], Jennifer M. Comstock[5], Julien Delanoë[2], Min Deng[6], Maureen Dunn[7], Robin J. Hogan[8], Dong Huang[7], Michael P. Jensen[7], Gerald G. Mace[9], Renata McCoy[1], Ewan J. O'Connor[8,10], David D. Turner[11], Zhien Wang[6]

1. Lawrence Livermore National Laboratory, Livermore, CA, USA

2. The Laboratoire Atmosphère, Milieux, Observations Spatiales, Guyancourt, FR

3. The Centre for Australian Weather and Climate Research, Melbourne, Victoria, AU

4. Cooperative Institute for Research in Environmental Science, University of Colorado and NOAA Earth System Research Laboratory, Boulder, CO, USA

5. Pacific Northwest National Laboratory, Richland, WA, USA

6. University of Wyoming, Laramie, WY, USA

7. Brookhaven National Laboratory, Upton, NY, USA

8. University of Reading, Reading, UK

9. University of Utah, Salt Lake City, UT, USA

10. Finnish Meteorological Institute, Helsinki, FI

11. NOAA National Severe Storms Laboratory, Norman, OK, USA

Key Words: Cloud retrievals, Uncertainties, Effective Radius, Liquid Water Content, Ice Water Content

Abstract: Accurate observations of cloud microphysical properties are needed for evaluating and improving the representation of cloud processes in climate models. However, large differences are found in current cloud products retrieved from ground-based remote sensing measurements using various retrieval algorithms. Understanding the differences is an important step to address uncertainties in the cloud retrievals. In this study, an in-depth analysis of nine existing ground-based cloud retrievals using ARM remote sensing measurements is carried out. We place emphasize on boundary layer overcast clouds and high level ice clouds, which are the focus of many current retrieval development efforts due to their radiative importance and relatively simple structure. Large systematic discrepancies in cloud microphysical properties are found in these two types of clouds among the nine cloud retrieval products, particularly for the cloud liquid and ice effective radius. It is shown that most of these large differences have their roots in the retrieval algorithms used by these cloud products, including the retrieval theoretical bases, assumptions, as well as input and constraint parameters. This study suggests the need to further validate current retrieval theories and assumptions and even the development of new retrieval algorithms with more observations under different cloud regimes.

1. Introduction

Globally, clouds cover more than 65% of the earth [Rossow and Schiffer 1999; Wylie et al. 2005]. Their properties are directly linked to the surface radiation budget through their solar and infrared radiative effects [Ramanathan 1987, Ramanathan et al. 1989]. However, the treatment of clouds has remained one of the largest uncertainties in current climate models because the processes that control cloud dynamics and their macro- and micro-physics as well as the interaction between clouds and radiation are not well understood [IPCC 2007].

Improving cloud representation in climate models requires improved knowledge of these cloud processes through detailed cloud observations. Cloud microphysical properties can be directly measured by in-situ probes or sensors aboard research aircraft. Due to its high cost, however, aircraft data is usually only available over very limited locations and time periods such as during a few major field campaigns. Furthermore, there are still measurement uncertainties for these in-situ aircraft observations, which are usually from ice shattering, counting statistics in low number density clouds, and assumptions based on scattering functions. To obtain long-term continuous measurements of cloud properties, ground-based and space -borne remote sensors (e.g., radars, lidars, radiometers, etc.) are often used. Cloud microphysical properties can then be retrieved from these remote sensing measurements using various retrieval algorithms.

Using ground-based remote sensors and other instruments, the Department of Energy (DOE)'s Atmospheric Radiation Measurement (ARM) program has continuously monitored clouds, radiation, and their associated atmospheric states for over a decade at its primary research sites

spanning latitudes from tropical to Arctic. The goal of ARM is to better understand clouds and their interaction with radiation and improve cloud parameterizations in global climate models [Ackerman and Stokes, 2003]. Various cloud retrieval techniques [e.g. Mace et al. 1998, 2002; Wang et al. 2004; Turner 2005; Shupe et al. 2005; Deng and Mace 2006; Hogan et al. 2006a; Delanoë et al. 2007; Delanoë and Hogan 2008; Huang et al. 2009; Protat et al. 2010; Dunn et al. 2011] have been developed to meet this goal. These retrieval products provide valuable information on cloud properties. However, large differences have been found between these cloud retrieval products in earlier studies. For example, the inter-comparison studies conducted by Comstock et al. (2007) and Turner et al. (2007a) showed large cloud property differences between different retrievals for high level ice clouds and optically thin liquid clouds, respectively; and a comprehensive focus study done by Shupe et al. (2008) demonstrated large differences that existed in several retrievals for mixed-phase clouds. Most of these studies were based on a few limited cases over short time periods.

Understanding these differences in current cloud retrieval products is important for evaluating and constraining climate models. Cloud retrieval uncertainties may arise from instrument limitations, measurement errors, sampling errors, and assumptions used in the retrieval algorithm, as well as from errors in the input data and constraints used by different algorithms. In this study, we first document differences among the various cloud retrieval products and then try to understand what differences can be explained by the differences in the retrieval algorithms, assumptions, and input and constraint parameters. Our goal is to examine cloud property differences, illustrate the potential causes from the way they are retrieved, and explore potential

issues that need to be addressed. In contrast to earlier studies, our analysis is performed over a much longer time period for different cloud regimes so that statistical characteristics of the examined cloud retrievals can be explored. For this purpose, nine ground-based cloud retrieval products that are available over multiple years at the ARM Southern Great Plains (SGP), North Slope of Alaska (NSA), and Tropical Western Pacific Sites (TWP) are used in this study. Systematically documenting the differences among these retrieval products will also help scientists to better understand how to use the data.

In section 2, we briefly summarize the ARM measurements and the nine ground-based cloud retrieval products used in this study. Section 3 shows how the different cloud properties retrieved from various algorithms are affected by their algorithm differences, as well as differences in their input and constraint parameters. In section 4, a statistical analysis based on multi-year data is carried out to study the systematic differences between cloud retrieval products. A summary of findings and a brief discussion of future studies are given in section 5.

2. Ground Based Cloud Retrievals

Table 1 lists the nine ground-based cloud retrievals that are used in this study along with their primary investigator (PI) contact information and primary references. For each of the five ARM permanent research sites, i.e., SGP, NSA, TWP Manus Island (TWPC1), TWP Nauru Island (TWPC2), and TWP Darwin (TWPC3), there are multiple cloud retrieval products from different research groups. Note that not all of them are available for all the sites and all types of clouds. The exception is the MICROBASE product, which is the ARM baseline cloud retrieval value-

added product (VAP) and contains all cloud properties for all cloud conditions over the five sites. These cloud retrieval products have been widely used in various studies to validate and improve cloud microphysical parameterizations in climate and weather forecast models as well as to evaluate satellite observations. For example, Xie et al. (2005) and Xu et al. (2005) used the MICROBASE data to examine model simulated cloud microphysical properties of midlatitude frontal clouds in multi-model intercomparison studies. Klein et al. (2009) used both SHUPE_TURNER and WANG cloud products for assessment of model simulations of single-layer mixed-phase clouds in the Arctic. Illingworth et al. (2007) applied the CLOUDNET process to assess numerical weather forecast models. Dong et al. (2008) used the MACE retrieval products to assess satellite cloud remote sensing.

The nine cloud retrieval products are mainly based on the measurements from the millimeter-wavelength cloud radar (MMCR), microwave radiometer (MWR), micropulse lidar (MPL), and the atmospheric emitted radiance interferometer (AERI). The MMCR [Moran et al. 1998] is a zenith-pointing radar that operates at a frequency of 35 GHz and provides measurements of radar reflectivity (Z), Doppler velocity (V_d) and spectral width (σ_d) with a vertical resolution of 45 m and a maximum possible measureable height of 20 km. The MMCR measurements are widely used by most retrieval techniques (Z based, Z-V_d based and Z-V_d-σ_d based) for deriving vertical profiles of particle size and water content for both liquid and ice clouds. Liquid water path (LWP) from microwave radiometer retrieval [MWRRET, Turner et al. 2007b, Turner 2007], with uncertainties of 20-30 g/m^2, is used by many of the retrieval products (MICROBASE, MACE, SHUPE_TURNER, COMBRET) as a constraint or input for deriving cloud liquid water

content (LWC). Slightly differently, CLOUDNET retrieves LWP from MWR with a method developed by Gaussiat et al. (2007) which shows the retrieved LWPs have uncertainties less than 10 gm^{-2} for LWP<20 gm^{-2} and less than 10% for LWP>20 gm^{-2}. WANG uses MWR LWP retrievals by Wang [2007] which shows LWP uncertainties less than 10 g/m^2 at NSA. For the LWP retrieval from MWR, MWRRET, CLOUDNET, and WANG all incorporate additional information (such as ceilometer and radiosonde profiles) to recognize clear sky conditions where LWP should be zero, with the CLOUDNET method using optimal estimation methods to continuously recalibrate slow drifts in the brightness temperatures. The MPL measurements are generally used to determine the altitude of clouds, particularly the cloud base. Moreover, the backscatter profile provided by MPL is also used by several algorithms (WANG, COMBRET, and VARCLOUD) for the retrieval of visible extinction coefficients. The AERI measures the absolute infrared spectral radiance of the sky directly above the instrument with a spectral resolution of 1.0 cm^{-1}. The AERI surface spectral radiance, particularly at the atmospheric window of 8-12 um, is often used by optimal estimation retrieval techniques (AERI-based retrieval hereafter) that iteratively minimize the difference of radiance between measurements and radiative transfer model simulations to get the cloud microphysical properties [Mace et al. 1998; Wang et al. 2004; Turner 2005]. The AERI-based retrieval techniques are used in the MACE, SHUPE_TURNER and WANG products.

For different cloud regimes measured by various remote sensors, the cloud retrieval algorithms vary widely. Particularly, different algorithms are typically used to retrieve cloud properties based on the cloud phase (ice, liquid, mixed). Actually, even for the same remote sensing

measurements, the cloud retrievals could be different because of their different assumptions. Table 2 provides a summary of the retrieval methods used in the nine ground-based cloud retrieval products, including cloud types to which the retrieval algorithms are applied, retrieval theories, major assumptions, major retrieval equations, and required inputs. Brief explanations of the symbols and abbreviations in Table 2 are given in the appendix A. Main features of the nine retrieval products are briefly summarized in Appendix B. More detailed descriptions are given in a technical report (Zhao et al. 2011, http://www-pcmdi.llnl.gov/ARM/cred/credreport.pdf).

Besides the algorithm details described in Appendix B, the nine retrieval products differ from each other in many other issues, like the cloud phase classification, cloud masks, radar reflectivity calculation and threshold values used in the algorithm, and the treatment of drizzle. For example, MICROBASE uses a simple temperature based phase classification method, in which the clouds are classified as liquid, mixed and ice for the temperature range of $T \geq 0^{\circ}C$, $-16^{\circ}C < T < 0^{\circ}C$, and $T \leq -16^{\circ}C$, respectively, while SHUPE_TURNER and COMBRET use an advanced cloud phase classification method developed by Shupe (2007) which is based on the combination of radar, lidar, LWP and temperature. For the radar reflectivity, instead of using the value-added product of the Active Remotely Sensed Cloud Locations (ARSCL), MACE and CLOUDNET do their own radar moments processing methods. Thus, it is likely that the cloud retrieval products are using slightly different radar reflectivity values. For the treatment of drizzle, some retrieval products (e.g. COMBRET) have classified drizzle from clouds while others just ignore the presence of drizzle (e.g. MICROBASE). Actually, many low warm (particularly thick) clouds contain drizzle [Kubar et al. 2009], leading to different errors in

different algorithms. These errors are hard to evaluate and not discussed in this paper, but should be kept in mind as factors that can cause differences between retrieval products. It should also be noted that the combination of radar and lidar will see more ice clouds than radar only. All these differences could be classified as the differences in the cloud retrieval inputs.

In practice, various assumptions need to be made within these retrieval algorithms, including assumptions about the particle size distributions (PSD), ice crystal habit, and ice density (ρ_i). Different algorithms often use different assumptions because of high natural variability of cloud properties and due to different interpretations of in-situ observations. As shown in Table 2, all retrieval algorithms assume a log-normal PSD for liquid particles but they assume either an exponential (e.g. MICROBASE, DENG and part of MACE and SHUPE_TURNER) or a (modified) gamma PSD (e.g., CLOUDNET, WANG, COMBRET and part of MACE and SHUPE_TURNER) for ice particles. The assumption for ice crystal habit varies between different retrievals and different locations. Most radar-based retrieval algorithms, like MACE and DENG, also assume applicability of Rayleigh scattering theory, or that the radar wavelength is large compared to the scatters resulting in the 6^{th} power law relationship between particle size and radar reflectivity.

For ice r_e, the definition might be different for the cloud products with non-spherical ice crystal habit assumption [McFarquhar and Heymsfield 1998], and we need to convert them into the same definition for the following intercomparison studies. For the nine cloud products studied

here, MICROBASE, SHUPE_TURNER, DENG, RADON, and VARCLOUD have used the definition of

$$r_e = \frac{3IWC}{4\rho_i A_c} \quad (1)$$

where ρ_i and A_c are ice density and projected area associated with the size distribution. Note that DENG, RADON and VARCLOUD directly use this equation with their derived ice extinction coefficient while MICROBASE and SHUPE_TURNER uses a T-based and a Z-based parameterization method, respectively. MACE has used the effective spherical radius defined in terms of the total volume of the distribution to the total area [Mace et al. 1998] and we simply assume it is comparable to the definition of Eq. (1) in this study. Differently, COMBRET and WANG use a generalized effective diameter D_{ge} [Fu 1996]. In this study, we convert D_{ge} to the ice r_e defined in Eq. (1) using an equation [Eq. 3.12 in Fu 1996]

$$r_e = D_{ge} * 0.6495 \quad (2)$$

The errors in this conversion are not discussed and simply assumed as negligible.

Differences in the theories, assumptions, inputs, and constraints used in the algorithms that might result in significant variability among the final retrieval products will be examined in the following sections. To simplify the issue, in this study, we will focus our analysis on two simple types of clouds, boundary layer overcast clouds and high level ice clouds, to which most retrieval algorithms listed in Table 2 can be applied.

Figure 1 shows current data availability for the nine ground-based cloud retrieval products using ARM measurements. There are three to six different retrieval products available for multiple years at each site. For example, we have multiple retrievals available particularly for the period between 2002 and 2007 at SGP, NSA, TWPC1 and TWPC2, and the period between 2005 and 2008 at TWPC3. To facilitate the following intercomparisons, all the retrievals have been converted to a uniform format with hourly time resolution and 45 m vertical resolution. The same cloud samples (same height and time) are used for comparing different retrieval products.

3. Differences between Cloud Retrievals

Section 2 described the major features of the retrieval algorithms for the nine ground-based retrievals used in this study. In this section, we will demonstrate how the differences in these retrieval algorithms impact their final retrieval products. Potential issues with inconsistent input data and constraints used by these retrievals are also discussed.

3.1 Differences due to Retrieval Algorithms

Most ground-based retrieval techniques are developed specifically for stratus or cirrus clouds due to their radiative importance and relatively simple structures. Even for these two types of clouds, earlier studies showed that large differences exist in retrieved cloud properties among different retrieval algorithms [Turner et al. 2007a, Comstock et al. 2007]. Different from the evaluation or sensitivity study with in-situ observations and radiation closure test by Comstock et al. (2007) and Turner et al. (20071a), here we do not intend to evaluate the quality of the cloud retrievals

from different algorithms but want to understand the differences between cloud retrieval products from their algorithm details with long term data. For simplicity, we examine all single-layer high level ice clouds and boundary layer overcast clouds.

235

3.1.1 Boundary Layer Overcast Clouds

As shown in Table 2, the retrieval techniques usually differ from each other in their fundamental theories and assumptions. Below we try to understand how these differences impact their retrieval results for cloud liquid properties in both liquid phase and mixed-phase clouds. Note
240 that the boundary layer overcast clouds discussed in this study are defined as single layer liquid and mixed-phase clouds with tops below 2 km and hourly cloud fraction over 90%. The cloud boundary, cloud layer and cloud fraction are from ARM climate modeling best estimate (CMBE, Xie et al. 2010), which is based on cloud frequency of occurrence from the vertically pointing MMCR and MPL.

245

a. Liquid Phase Clouds

Boundary layer clouds are generally in liquid phase at the SGP and TWP sites while a large fraction are mixed-phase at the NSA site. There are five retrieval products that provide cloud liquid properties for pure liquid clouds. They are MICROBASE, MACE, CLOUDNET,
250 SHUPE_TURNER, and COMBRET. These cloud products use either optimal estimation method or empirical parameterization method.

For liquid r_e, both MACE and SHUPE_TURNER use a radiance based optimal estimation method for optical thin clouds and a radar reflectivity based parameterization method for optical thick clouds. The radiance based optimal estimation method makes use of the optimal match of surface shortwave or infrared (IR) radiance between measurements and calculations. The radar based parameterization method makes use of the 6^{th} power law relationship between particle size and radar reflectivity, which most heavily weights the large droplets. We cannot conclude if there are any biases for liquid r_e in MACE and SHUPE_TURNER considering multiple degrees of freedom that could impact the retrieval. In contrast, the MICROBASE and COMBRET liquid r_e is obtained using the power law relationship between LWC and liquid r_e based on derived LWC and a log-normal particle size distribution. There is also a notable difference for the derivation of liquid r_e between MICROBASE and COMBRET. MICROBASE derives cloud liquid r_e using LWC scaled with MWRRET LWP and a constant number concentration (N) of 200 cm^{-3} for all sites, while COMBRET calculates the liquid r_e using LWC before the scale of MWRRET LWP and a constant N of 100 cm^{-3} for TWP sites. N=200 cm^{-3} in MICROBASE is generally a reasonable assumption for land area at SGP. However, for NSA and TWP sites, this number might be too large to make liquid r_e underestimated. In comparison, N=100 cm^{-3} for TWP sites might be a reasonable assumption since the clouds are more close to those over ocean. Therefore, we expect liquid r_e from MICROBASE is smaller than that from SHUPE_TURNER at NSA, while it is hard to expect the difference between MICROBASE and MACE at SGP and the difference between MICROBASE and COMBRET at TWP.

Figure 2a, b and c show the differences in liquid r_e for the same liquid only clouds during the period from May through November in 2004 between MACE and MICROBASE at SGP,

SHUPE_TURNER and MICROBASE at NSA, and MICROBASE and COMBRET at TWPC3, respectively. Note that hourly averaged cloud properties for which all algorithms compared have valid values at the same time and height are used. Figure 2a shows slightly smaller liquid r_e in MICROBASE than MACE at SGP, which might be related to their different retrieval inputs. Figure 2b shows that liquid r_e in MICROBASE is systematically less than that in SHUPE_TURNER, which should be partly associated with the number concentration assumption in MICROBASE. In contrast, Figure 2c shows a similar r_e distribution between MICROBASE and COMBRET from May through November 2007 at TWPC3 since they use similar retrieval algorithms. The slight difference in cloud liquid r_e between MICROBASE and COMBRET might be related to a combination of their differences in the LWC used for liquid r_e calculation and the assumption in droplet number concentration.

For the retrieval of LWC, LWP derived from MWR is often used either as a constraint or as an input parameter by most algorithms. However, the algorithm used to retrieve LWP is not always the same for these cloud products. Even for the same LWP constraint, the LWC can follow different vertical structures due to algorithm differences. From the theoretical equations used in the retrieval algorithms as shown in Zhao et al. (2011), we know that the vertical gradients of LWC in MICROBASE, COMBRET and SHUPE_TURNER (liquid only clouds) are proportional to $Z^{1/1.8}$ and the LWC in MACE is proportional to $Z^{1/2}$, while the LWC in CLOUDNET and SHUPE_TURNER (mixed-phase clouds) follows an adiabatic gradient determined based on temperature and moisture profiles. For pure liquid clouds, we can expect

that MICROBASE, MACE, and CLOUDNET have different vertical distributions, and that MICROBASE, COMBRET and SHUPE_TURNER have similar vertical distributions.

Figure 3a and 3b show the vertical distributions of mean LWC at each height for these retrieval products for the same clouds from May through November in 2004 at SGP and NSA, respectively. The LWC vertical distributions shown in Figure 3a and 3b do demonstrate the theory related differences (MICROBASE, MACE and CLOUDNET) and similarities (MICROBASE and SHUPE_TURNER) discussed above. Note another contribution to the difference of LWC between MACE and MICROBASE is their difference in radar reflectivities as described in section 2. The large offset in retrieved LWC values between MICROBASE and MACE or CLOUDNET at SGP (Fig. 2a) should be mainly caused by their different LWP constraints.

The relationship between LWC and liquid r_e varies among the retrieval products. Theoretically,

$$LWC = \int (\frac{4\pi\rho_l r^3 N(r)}{3})dr \qquad (3)$$

where ρ_l is the water density, r is droplet size, and N(r) is droplet size distribution. With an assumed (like log-normal or gamma) particle size distribution, if N is assumed (MICROBASE and COMBRET), LWC and liquid r_e follow a power-law relationship. If LWC and r_e are derived independently (MACE, SHUPE_TURNER) with no assumption on N, the two variables might show unexpected relationships. Figure 4 shows the relationship between LWC and liquid r_e for liquid cloud products at SGP, NSA and TWPC3, in which the red lines are the fitting lines with a

2^{nd} order polynomial function. LWC and liquid r_e in MICROBASE follow the relationship expressed in Eq. (3) for a constant N (200 cm^{-3}). In contrast, LWC and liquid r_e are determined independently in MACE and SHUPE_TURNER and demonstrate a poor correlation with almost no relationship. COMBRET (Figure 4f) shows a much weaker power relationship between LWC and liquid r_e compared to that for MICROBASE. Although COMBRET uses a similar retrieval algorithm as MICROBASE, it first calculates LWC, then liquid r_e, and finally scales the integrated LWC to match the MWRRET LWP. In another word, the final LWC is no longer consistent with the LWC used to derive liquid r_e, which is why the power relationship does not show strongly.

b. Mixed-phase Clouds

Mixed-phase clouds are frequently observed at NSA [Shupe 2011] and their liquid component has a large impact on cloud radiative effects [Shupe and Intrieri 2004]. With a small amount of LWP (<100 g/m^2) [Lin et al. 2003; Shupe et al. 2005], most Arctic clouds have their radiative properties sensitive to microphysical properties. Below we discuss the differences among mixed-phase cloud microphysical properties retrieved at the ARM NSA site.

Associated with the retrieval theoretical basis, clear differences exist in the vertical variations of cloud properties. As shown in Table 1, there are 3 available cloud retrieval products for boundary layer mixed-phase cloud properties at NSA, which are MICROBASE, SHUPE_TURNER and WANG. Figure 5a and 5b show the vertical structure of hourly averaged liquid r_e from MICROBASE and SHUPE_TURNER for mixed-phase clouds. The cloud liquid r_e

in WANG is not shown here because it is layer averaged r_e. For the mixed-phase clouds, MICROBASE obtains the cloud liquid r_e based on radar reflectivity (Z) and cloud temperature (T) using

$$Z_{liq} = (1 + T/16)Z \quad (4)$$

$$r_e = \left(\frac{3(N_d Z_{liq}/3.6)^{1/1.8}}{4\pi\rho_l N \exp(9\sigma_x^2/2)} \right)^{1/3} \exp(2.5\sigma_x^2) \quad (5)$$

where T is between -16 and 0 degree C. In contrast, SHUPE_TURNER derives the layer averaged cloud liquid r_e using AERI-based optimal estimation method for optical thin clouds, derives the profiles of cloud liquid r_e using Z-based parameterization method for all-liquid layers, and sets a climatology value of 8 um for those that cannot be retrieved. As shown in Fig. 5a, the decrease of cloud temperature with height results in a decrease of liquid r_e with height in MICROBASE for period between October 9 and October 15, 2004 while the hourly average of cloud liquid r_e from SHUPE_TURNER generally increases or stays constant with height within a layer (Fig. 5b). Over the same period, aircraft measurements in the Arctic from the Mixed-Phase Arctic Cloud Experiment (M-PACE) have shown a typical vertical structure of single-layer mixed phase clouds in which the liquid r_e increases with height [Verlinde et al. 2007]. This feature has also been observed in other field campaigns in the Arctic region, like the First ISCCP (International Satellite Cloud Climatology Project) Regional Experiment/Surface Heat Budget of the Arctic (FIRE-ACE/SHEBA, Hobbs et al. 2001). Figure 5 also shows the different phase classification. For example, for the ice beneath liquid cloud bases in SHUPE_TURNER, MICROBASE has classified them as liquid or mixed.

The retrieved cloud liquid microphysics, particularly the cloud liquid r_e, also exhibits a notable difference in the probability density functions. As an example, Figure 6 shows that the liquid r_e retrieved from both SHUPE_TURNER and WANG is systematically larger than that from MICROBASE for single-layer, mixed-phase boundary layer clouds. As indicated earlier, the large droplet number concentration assumed at NSA in MICROBASE might make liquid r_e underestimated. Another possible reason is that the radar reflectivity for mixed-phase clouds is less sensitive to the droplet sizes but more sensitive to the large ice particles. The estimation of radar reflectivity for the cloud droplets in Eq. (4) as MICROBASE uses may not be suitable, causing the retrieved liquid r_e to be systematically smaller than the others. Without considering the adopted climatological value (r_e=8 um), the cloud liquid r_e retrieved by SHUPE_TURNER is in a similar range to that retrieved by WANG.

There are some other assumptions held in current retrievals of the boundary layer overcast cloud properties, such as the horizontal homogeneity assumption and the log-normal particle size distribution (PSD) assumption. These assumptions also introduce uncertainties to the cloud retrievals. However, since these assumptions are similar for all the retrieval algorithms examined in this study except their difference in the time resolution, they cannot be the main reason for the large differences found in these retrievals and therefore are not discussed here.

3.1.2 High Level Ice Clouds

The high level ice clouds examined in this study refer to single-layer ice clouds with hourly cloud fraction over 90% and cloud bases above 4 km, 5 km and 6 km at NSA, SGP and TWP, respectively. Similar to the algorithms used for the stratus clouds, the ice cloud retrieval techniques can also be classified into two categories: the forward or optimal estimation approach (MACE, DENG, VARCLOUD, and RADON) and the empirical parameterization method (MICROBASE, MACE, CLOUDNET, SHUPE_TURNER, and COMBRET). Note that the MACE cloud product includes retrievals from both categories. The forward approach uses theoretically based equations with certain assumptions to derive cloud properties. In contrast, the empirical parameterization method uses empirical regression equations based on available aircraft observations. In general, there are more unknowns and therefore more assumptions that need to be made for ice clouds than liquid clouds due to their complexity in bulk density, particle shape, and particle formation processes. Moreover, the retrieval of ice cloud properties is hampered by a lack of constraint on the total IWP. These extra limitations could result in larger retrieval uncertainties for high level ice clouds than for the boundary layer overcast clouds.

We first emphasize the cloud retrieval differences related to the fundamental basis used in the retrieval algorithms. It is seen from Table 2 that the high level ice clouds are retrieved using the radar-based retrieval methods by most algorithms (MICROBASE, MACE, CLOUDNET, DENG, SHUPE_TURNER, COMBRET, RADON). Some of them also use the surface spectral radiance (MACE, SHUPE_TURNER) or lidar extinction coefficient (COMBRET, VARCLOUD). Note that results from WANG are not presented in this section since the product currently only includes mixed-phase cloud properties.

Figure 7 shows large discrepancies in the retrieved ice cloud properties. For all ARM sites, ice r_e from MICROBASE is generally smaller with a narrower range than that from others. This is mainly because the MICROBASE ice r_e retrieval is based on cloud temperature (T) using [Dunn et al. 2011]

$$r_e = (75.3 + 0.5895T)/2 \quad (6)$$

At the maximum 0°C for ice clouds, MICROBASE has a maximum r_e of 37.7 um, demonstrating a very limited range. On the other hand, MACE, DENG, and SHUPE_TURNER make use of the 6^{th} power relationship between cloud radar reflectivity and particle size, and are therefore more sensitive to large particles compared to MICROBASE. Interestingly, ice r_e from DENG at NSA and from RADON at TWPC3 is even smaller than that from MICROBASE. The small ice r_e in DENG at NSA might be associated with the parameters (e.g. particle mass-length relationship) used for clouds at NSA, which has not been explicitly evaluated and might have relatively large uncertainties. The small ice r_e in RADON at TWPC3 might be related to the fact that the ice particle density-diameter relationship is retrieved for each cloud from the fall speed – radar reflectivity relationship rather than assumed the same for all clouds, which is a feature in RADON that makes the RADON based radiation calculation have a good agreement with the ground-based radiation observation. For COMSTOCK, VARCLOUD, and WANG, a unique feature is that they make use of both radar and lidar measurements. Correspondingly, VARCLOUD and COMSTOCK show similar ranges of ice r_e at TWPC3 in Figure 7. Due to the common use of radar reflectivity in MACE, DENG, SHUPE_TURNER, COMSTOCK, and VARCLOUD, Figure 7 shows high correlations in ice r_e among them.

425

The cloud property differences associated with the fundamental basis used in the ice retrievals can also be illustrated from the relationship between IWC and ice r_e. Figure 8 shows a clear power law relationship between IWC and ice r_e for MACE, SHUPE_TURNER, and DENG, and a relatively weaker power law relationship for MICROBASE, COMBRET, RADON and
430 VARCLOUD for clouds during the period between May and November in 2004 at NSA and SGP and in 2007 at TWPC3. The IWC and ice r_e from MACE, SHUPE_TURNER and DENG are related in this way because they are derived from radar reflectivity using parameterization methods. Note that MACE shows two patterns of relationships between IWC and ice r_e since it uses an optimal estimation retrieval method for thin cirrus (small ice r_e) and a parameterization
435 method for thick ice clouds. In contrast, the IWC and ice r_e from MICROBASE are derived using parameterization methods based on radar reflectivity and cloud temperature, respectively, making their correlation weaker. IWC and ice r_e in VARCLOUD are related through the visible extinction coefficient using an optimal estimate, resulting in a weak power law relationship between IWC and ice r_e. Interestingly, MICROBASE, COMBRET, and RADON demonstrate
440 that IWC increases first and then decreases with ice r_e at TWPC3. Furthermore, COMBRET shows a decrease instead of increase of IWC with ice r_e for the period of May through November in 2004 at TWPC2 (not shown here). The reasons for the relationships found between IWC and ice r_e in MICROBASE and RADON are not clear while the relationship for COMBRET could be largely related to the cloud retrieval input which is discussed in Section 3.2.

445

We next examine how the cloud retrieval differences are caused by uncertainties in defining various empirical parameters used in these algorithms. The regression equations and empirical parameters are often derived based on the limited short period in-situ measurement data, which may not be valid globally due to the complexity of the clouds. The different parameters used by various retrieval algorithms will cause discrepancies in the retrieved cloud properties. For example, many ice cloud retrieval algorithms (e.g. MICROBASE, MACE, and SHUPE_TURNER) use $IWC=aZ_e^b$ to determine IWC. Here Z_e is water equivalent radar reflectivity. However, parameters a and b are defined differently in different retrieval techniques. In MICROBASE and MACE, a=0.097 and b=0.59. In SHUPE_TURNER, a is a tunable parameter dependent on time of year which roughly lies between 0.05 (summer) and 0.12 (winter) and b=0.63. These parameter differences will lead their differences in retrieved IWC, most possibly making IWC from SHUPE_TURNER less than that from MICROBASE or MACE. For example, for a winter (summer) time value of a=0.097 (0.06) and for a cloud with -30 dBZ radar reflectivity, the IWC in SHUPE_TURNER is about 24% (53%) less than that in MICROBASE.

Next, we discuss the retrieval differences associated with the ice crystal habit assumptions. For most ice cloud retrieval algorithms, empirical power law relationships between particle mass, ice bulk density, or terminal velocity and particle maximum dimension length, are often adopted. Unfortunately, these power-law relationships are highly sensitive to the assumed ice crystal habits. As indicated by Comstock et al (2007), for each ground-based ice cloud retrieval technique examined, an assumption concerning the ice crystal shape is made. For example,

MACE uses a hexagonal column shape (Mace et al. 1998) and a bullet rosette shape (Mace et al. 2002) for ice particles in cirrus at SGP site, MICROBASE assumes planar polycrystals for ice particles at all sites, while WANG, COMBRET (except clouds retrieved with radar only) and DENG assume a hexagonal shape for ice particles at the NSA site, three TWP sites, and all sites, respectively. However, in reality clouds usually have a mixture of ice particles with different shapes which vary vertically [Heymsfield and Iaquinta, 2000] and have complicated mass-length relationships. Various field observations and lab studies [McFarquhar and Heymsfield, 1996; Korolev et al., 1999; Noel et al., 2004; Verlinde et al., 2007; McFarlane and Marchand, 2008; Bailey and Hallet, 2009] have shown a high geographic and temporal variability of ice crystal habits. The necessary but simplified ice crystal habit assumptions can have a large impact on the retrieved cloud microphysical properties. For example, a sensitivity study conducted by Mace et al. (2002) showed that a difference with a factor of up to 4 in IWC could be caused by the ice crystal habit assumption for one particular cloud retrieval method. Wang and Sassen (2002) indicated that different particle mass-length assumptions could change the Z/IWC relationship by up to 50%. Therefore, the differences in ice crystal habit assumptions are partially responsible for the large discrepancies found between retrievals, such as the ice r_e differences between MICROBASE, MACE, DENG, and COMBRET shown in Figure 7. The exact impact of different ice crystal habit assumptions on each retrieval algorithm needs further sensitivity analysis, which is beyond the current study and will be done in the future.

Finally we talk about the impacts of different particle size distribution (PSD) assumptions on cloud retrievals. A common assumption is that a single PSD is sufficient to determine the

scattering properties of the ice crystals within the cirrus layer [Mace et al., 2002]. Gamma (or modified gamma) and exponential PSD are the two widely used unimodal PSD assumptions for current ice cloud retrieval algorithms. But, bi-modal distributions have been found for a large fraction of cirrus clouds [Mitchell et al. 1996; Mace et al. 2002; Zhao et al. 2011]. Recent field measurement during the Small Particles In Cirrus (SPARTICUS) campaign at SGP suggests that the bimodal PSD is not always better than the unimodal PSD to fit the measured particle size distributions [Schwartz and Mace 2011]. Therefore, it is not clear that any given PSD assumption is better than another in a generic sense. However, there is no doubt that different assumption in PSD leads to different retrievals. For example, it is obvious that more particles are concentrated in the small size area, then that smaller r_e is retrieved with an exponential PSD in comparison to those retrieved with a gamma PSD [Deng and Mace 2006].

3.2 Impacts of the Inputs and Constraints Used in Cloud Retrievals

Another source of uncertainty in these retrievals is from the use of inconsistent inputs and constraints. Information on the cloud boundaries, cloud phase, and hydrometer classification must be derived before cloud retrievals are applied. Earlier studies showed that differences in the input and constrained variables used in different algorithms can have a large impact on the retrieved cloud properties [Dunn et al. 2009; Huang et al. 2011].

Cloud boundaries can be derived from various remote sensors or a combination of different sensors such as ceilometers, MPL, and MMCR with specific criteria. The difference in deriving the cloud boundaries between different algorithms can make the retrieved cloud properties

disagree considerably with each other. Similarly, different hydrometer classification could also results in large discrepancies in the retrieved microphysical properties, like the difference between drizzle and cloud droplets. Unfortunately, as described in Section 2, these cloud retrieval products are not derived by using a uniform cloud phase and hydrometer classification method. Although we have limited the inter-comparison of cloud microphysical properties among the cloud products in this study with the same cloud phase and cloud location, the differences in the determination of cloud boundaries can still contribute to their discrepancies in the cloud microphysical properties, particularly for LWC. As mentioned earlier, another important but often different input/constraint parameter is LWP, which has been derived from MWR by different methods.

To illustrate these issues, Figure 9 shows the cloud LWP and ice water path (IWP) along with LWC and IWC at heights of 1000 m, 2000 m and 3000 m for October 2004 at SGP. It shows clear differences in cloud boundaries (e.g. day 278, 288, 293 and 297) and cloud phases (e.g. day 278 at 3 km height and day 290 at 1 km and 2 km). For example, MICROBASE and MACE identify clouds down to (or below) 1 km while CLOUDNET finds the cloud base above 2 km on day 278. Similarly, MICROBASE and MACE classify these clouds as liquid while CLOUDNET classifies them as ice on day 290 at 2 km height. Figure 9 also shows a clear difference in LWP among all three retrieval products for some periods (e.g. day 294).

Besides the cloud boundaries, cloud phase, and hydrometer classification, uncertainties and problems in other inputs can also cause errors in the cloud retrievals and then result in

differences in the cloud retrieval products. For example, the decreasing IWC with ice r_e for COMBRET in Figure 8 is most possibly caused by an issue that multiple scattering in the lidar signal near cloud top causes an overestimation of the extinction. It has been found that when the optical depth is smaller and the multiple scattering is less, IWC is positively correlated with ice r_e in COMBRET. But for thicker clouds which tend to dominate the tropics, negative correlation between IWC and ice r_e is often resulted from the lidar extinction near cloud top.

4. Statistical Analysis of ARM Cloud Retrievals

Section 3 has discussed the implications of retrieval algorithm differences in theoretical basis, assumptions, inputs and constraints, and shown their possible impacts on the differences in retrieved cloud properties. In this section, we will use multi-year data between 2002 and 2007 at SGP, NSA, TWPC1, and TWPC2, and between 2005 and 2008 at TWPC3 to examine differences in the probability distribution functions for the cloud properties and show a statistical summary of the correlations and differences among the cloud retrieval products.

4.1 Probability Distribution

In this subsection we examine the probability distribution function of cloud properties at SGP, NSA and one TWP site (TWPC3) for all cloud retrieval products to see if the differences found in section 3 are statistically robust. For each site, only the clouds that all applicable retrieval products have valid values are considered in this subsection. To better compare these products, we classify them into thin and thick clouds. Turner (2005) have shown that AERI-based optimal

estimation method is only valid for thin clouds with the optical depth (τ_l) less than 6 and Comstock et al. (2007) have used an optical depth (τ_i) of 0.3 to classify optical thin and thick ice clouds. Unfortunately, we do not have independent measurements of the cloud optical depths for all five ARM sites. Instead, we use the cloud geometric depth (ΔH) determined from CMBE cloud fraction to classify thin and thick clouds. The cloud geometric depth can be related to the cloud optical depth through

$$\tau_l = \frac{3LWC \bullet \Delta H}{2r_e} \quad (7)$$

$$\tau_i = 0.065(IWC \bullet \Delta H)^{0.84} \quad (8)$$

where LWC and IWC are in g/m^3 and ΔH is in m. The empirical equation for ice optical depth (Eq. 8) is from the study by Heymsfield et al. (2003). Considering typical values of liquid r_e=8 um, LWC=0.1 g/m^3 and ice IWC=0.01 g/m^3, the ΔH of 300 m and 600 m roughly correspond to optical depths of 6 and 0.3 for liquid and ice, respectively. Therefore, we classify geometric thin ($\Delta H \leq 300$ m) and thick ($\Delta H > 300$ m) clouds using 300 m for boundary layer overcast clouds, and classify geometric thin ($\Delta H \leq 600$ m) and thick ($\Delta H > 600$ m) clouds using 600 m for high level ice clouds.

Figure 10 shows the probability distributions of cloud liquid r_e and LWC from different cloud retrieval products for geometrically thin and geometrically thick boundary layer overcast clouds at 3 ARM fixed stations of SGP, NSA and TWPC3. Similarly, Figure 11 shows the statistical distributions of high level ice cloud properties. The numbers shown in the figures are the total cloud samples used for this statistical analysis at each site.

For both geometrically thin and thick clouds, Figure 10 and 11 show similar results as those found in Section 3. These similarities confirm that the large differences found between various retrieval products are not case dependent, but statistically robust. The robust differences indicate impacts from the combination of different retrieval techniques described in Section 2. The PDFs shown here also give rough ranges of cloud microphysical properties for different cloud retrieval products. For boundary layer stratus, liquid r_e mainly lies between 3 and 13 um for most retrieval products except for MICROBASE and WANG which have liquid r_e mostly within a range of 0 to 9 um and 7 to 17 um, respectively. For high level ice clouds, ice r_e mainly lies between 10 and 40 um for DENG at NSA and MICROBASE, between 5 and 60 um for RADON, and between 20 and 70 um for others. LWC in boundary layer clouds and IWC in high level ice clouds in these retrievals generally vary between 0 and 0.6 g m^{-3} and between 0 and 0.5 g m^{-3}, respectively. As a reference, observations from several major field campaigns [McFarquharg and Heymsfield 1996; Lawson et al. 2001; Dong et al. 2002; Heymsfield et al. 2004; McFarquhar et al. 2007; Yost et al. 2011] show that liquid r_e mainly varies between 3 and 25 um with mean values mostly in a range of 5 to 12 um and LWC mainly varies between 0.001 and 1 g m^{-3} with most mean values within a range of 0.1 to 0.3 g m^{-3} for stratus clouds. For cirrus clouds, the observations show IWC has a major a range of 0.0001 to 1 g m^{-3} with mean values varying from 0.001 to 0.1 g m^{-3}. The aircrafts measurements also show a large amount of small ice particles, which should be influenced by particle shattering in the process of measurement [McFarquhar et al. 2007; Protat et al. 2011]. Compared to these limited aircraft measurements, the cloud microphysical properties from most cloud products studied here lie within reasonable range statistically.

Evaluation studies about these cloud retrievals with a collection of available aircraft measurements will be done in the future.

600

4.2 Statistical Summary

In this sub-section we use the Taylor diagram [Taylor 2001] to examine the statistical relationship between retrieved cloud properties of different algorithms. We use MICROBASE as a reference (the black point marked 'M' in Figure 12) since MICROBASE is the ARM baseline
605 cloud retrieval value-added product and provides all cloud properties for all conditions at the five ARM sites. The Taylor diagrams in Figure 12 show correlations, centered root-mean-square (RMS) differences, and ratios of standard deviations for cloud liquid r_e, ice r_e, LWC, IWC, LWP and IWP between MICROBASE and the other retrievals. The centered RMS difference between these retrievals and MICROBASE is proportional to the distance to the point on the X-axis
610 identified as "M". As described by Taylor (2001), this diagram provides a concise statistical summary of how well the retrieval patterns match between MICROBASE and other retrievals. In Figure 12, we also use different colors to discriminate the difference in mean cloud properties between a retrieval and MICROBASE. The blue, black, yellow, and red colors indicate that the mean of the examined cloud properties retrieved from an algorithm are <70%, 70% -140%,
615 140% - 200%, and 200% - 400% compared to MICROBASE, respectively.

For boundary layer overcast liquid clouds, the correlation between MICROBASE and other cloud retrieval products is generally low. The differences in the correlation coefficients and centered RMS differences for liquid r_e and LWC shown in Figure 12a and Figure 12c are likely

620 associated with their differences in the retrieval theoretical basis and their differences in LWP (Figure 12e). For example, the LWC in MACE and SHUPE_TURNER is proportional to radar reflectivity for pure liquid clouds which is similar to MICROBASE, resulting in a smaller RMS difference relative to MICROBASE compared to CLOUDNET and WANG which are based on quasi-adiabatic profiles. It is noticed that the LWC derived from COMBRET, which uses a
625 similar retrieval algorithm to MICROBASE, has a very small correlation coefficient with MICROBASE and a large RMS difference. This is consistent with their difference in LWP, which also shows poor correlation and large RMS difference (Figure 12e). Figure 12 also demonstrates different mean cloud properties among the cloud products. Same as found previously, Figure 12a shows that cloud liquid r_e in MICROBASE is systematically smaller than
630 that in others, which again might be due to the droplet number concentration assumption and droplet radar reflectivity calculation used in MICROBASE. Figure 12c shows that the cloud LWC is less in MACE (SGP) and CLOUDNET (SGP and TWPC3) and is larger in WANG and COMBRET (TWPC2 and TWPC3) compared to MICROBASE. However, the average LWP is similar to MICROBASE for most cloud products except for WANG and COMBRET which give
635 smaller LWP. Considering the similarity of the mean values in LWP and that LWC has been scaled by the MWR LWP in all cloud products, the existing large differences in mean LWC among some retrieval products (e.g., WANG, COMBRET and MICROBASE) in Figure 12e suggest their differences in the determination of cloud boundaries.

640 In general, the ice cloud properties obtained from different cloud products have much higher correlation coefficient and smaller RMS difference than those for liquid clouds relative to

MICROBASE, particularly for IWC and IWP. Different from liquid cloud retrievals which are based on various measurements from AERI radiance, radar reflectivity, MWR LWP and temperature and moisture profiles, most ice cloud retrievals just make use of the radar, radar plus lidar, or radar plus temperature measurements. The commonality of radar data used by most ice cloud retrievals is likely the reason for the better correlations found in Figure 12b, d and f compared to the liquid cloud retrievals. For ice r_e in high level ice clouds, the correlation coefficient between MICROBASE and other cloud products mainly lies between 0.5 and 0.8. Respective to MICROBASE, the correlation is relatively weaker for SHUPE_TURNER and MACE compared to other retrievals. The reason might be that the ice r_e of thin ice clouds in SHUPE_TURNER and MACE are derived using radiance based optimal estimation method while other cloud products (also SHUPE_TURNER and MACE for thick clouds) are from radar (or radar-lidar) based retrievals. Figure 12b also shows that the ice r_e from temperature-based MICROBASE is smaller than from radar-lidar and radar-only based cloud retrievals at low (3 TWP sites) and middle (SGP) latitudes, except for from RADON. For IWC, MACE, CLOUDNET, and SHUPE_TURNER show a high correlation and a low RMS difference relative to MICROBASE, indicating their retrieved IWC has similar patterns. Actually, all four of these retrievals use a similar radar reflectivity based parameterization method. However, these techniques have used different parameters (like SHUPE_TURNER and MICROBASE) or have introduced other input (like T in CLOUDNET) to improve the retrieval, which might explain the difference in IWC between these retrievals. In contrast, COMBRET, DENG, RADON and VARCLOUD show larger averaged values and RMS differences in IWC relative to MICROBASE, which should be related to their different radar-lidar basis (COMRET and VARCLOUD) and radar Z-V_d basis (DENG and RADON). Based on the difference in the mean

values between IWC and IWP for the cloud retrieval products compared to MICROBASE shown in Figure 12d and 12f, we can see that MACE and CLOUDNET at SGP, SHUPE_TURNER and DENG at NSA, COMBRET at TWPC1, and CLOUDNET at TWPC3 have thicker ice cloud depths than MICROBASE; and RADON at TWPC3 has thinner ice cloud depths than MICROBASE.

5. Summary and Discussions

This study systematically examined the differences among nine cloud retrieval products (i.e., MICROBASE, MACE, CLOUDNET, DENG, SHUPE_TURNER, WANG, COMBRET, VARCLOUD and RADON) for boundary layer overcast clouds and high level ice clouds at the ARM SGP, NSA, and TWP sites. Following are the main findings.

For boundary layer liquid clouds, clear differences in liquid r_e and LWC have been found among cloud products associated with the differences in retrieval instrument basis (like AERI-based WANG and SHUPE_TURNER, and radar-based MICROBASE) and assumptions (like large droplet number concentration in MICROBASE at NSA and TWP, and negligence of drizzle in radar-based retrievals). Different vertical structure could also result from their retrieval basis and parameters, such as the LWC from radar based (MACE, MICROBASE, COMBRET, and SHUPE_TURNER) methods with different empirical parameters versus the LWC from adiabatic calculation (WANG, CLOUDNET, and SHUPE_TURNER). Note that SHUPE_TURNER obtains LWC using radar based method for liquid only clouds and adiabatic estimate for mixed-phase clouds.

For high level ice clouds, higher correlations in r_e and IWC are found between MICROBASE and other cloud retrieval products associated with their common use of radar reflectivity. The magnitude of the correlation coefficient is highly related to the similarity of their retrieval instrument basis (radar basis, radar-lidar basis, radar-T basis, and T basis). Similar to boundary liquid clouds, clear differences in ice r_e and IWC for high level ice clouds have been found among cloud retrieval products, which are associated with the differences in retrieval basis (like T basis in MICROBASE and Z, Z-σ_{ext}, or Z-T basis in others), parameters (like parameters in the regression equation for IWC between SHUPE_TURNER and MICROBASE), and assumptions (like mass-length relationships, density-length relationships, ice crystal habit, and particle size distribution). Note that the differences of cloud properties caused by differences in some assumptions have not been explicitly examined in this study, including the different ice crystal habit assumptions.

For the cloud retrieval input and constraint parameters (e.g., cloud phase, boundaries, and other inputs), we have briefly illustrated their differences among cloud retrieval products and showed the cloud property differences associated with them (like cloud boundaries and LWP) in the statistical analysis. Although we did not make much effort to discuss the impacts from different inputs and constraints considering most of them are easy to understand, we must acknowledge that cloud retrieval inputs and constraints are among the most important factors for the differences among cloud retrieval products.

In summary, this study has shown the large systematic differences between various cloud products and examined their possible reasons in the retrieval basis, assumptions, parameters, as well as the retrieval inputs and constraints. However, to quantify the effects from different factors and determine the best estimate of cloud properties under different conditions, further constraints of these retrievals with more observations and dedicated sensitivity analyses with different combination of the retrieval factors are desperately needed.

With a better understanding of different factors leading to differences in cloud properties between various cloud products, an integrated effort to quantify cloud retrieval uncertainties and develop a best estimate of cloud microphysical properties with error bars is desired. Developing a uniform input and constraint data file based on ARM value-added products, which provide a best estimate of these required fields, can help considerably reduce these differences as found in an earlier study [Dunn et al. 2010; Huang et al. 2011]. To address the uncertainty issue within current cloud retrievals, ARM is making an effort to assemble the ARM ground based cloud retrievals into a cloud retrieval ensemble dataset (CRED; Zhao et al. 2011), which could provide a rough estimate of uncertainties in these cloud retrievals based on current instruments and retrieval techniques provided that the algorithms were reasonably designed to retrieve cloud properties for a certain type of clouds. One problem with the current CRED is that the uncertainty in each of the ensemble members is unknown. To address this issue, one could generate an ensemble dataset for each of the algorithms by perturbing key parameters and/or changing key assumptions used in these selected retrieval methods. This will help improve our understanding of the uncertainty associated with each of these retrieval methods and provide

necessary information to further quantify the uncertainty using advanced statistical methods such as the Bayesian approach. Another idea is to create artificial datasets either from a model or just using idealized profiles and run the algorithms on these [McFarlane et al., 2002; Hogan et al., 2006b]. A carefully constructed comparison might be able to determine which algorithm is more accurate under which conditions, and what the effects of different assumptions are. Moreover, the accuracy of assumptions and parameters in the cloud retrievals can be evaluated and tested with more in-situ aircraft data and observed surface and top of atmosphere (TOA) radiative fluxes. In addition, with the knowledge of the strengths and weakness of retrieval algorithms based on sensitivity studies, it is possible to figure out the optimal technique for certain types of clouds under specific condition and then to develop a best estimated cloud properties data set by merging the optimal algorithms for all conditions together. In short, more research is needed to better understand and reduce the uncertainty in current cloud retrievals.

Acknowledgments. This study is supported by the DOE ARM and ASR programs. The LLNL IM release number is LLNL-JRNL-493852. Work at LLNL was performed under the auspices of the U. S. Department of Energy, Office of Science, Office of Biological and Environmental Research by Lawrence Livermore National Laboratory under contract DE-AC52-07NA27344. The contribution of Matthew D. Shupe is performed under the support by DOE grant DE-FG02-05ER63965. Work at PNNL was performed under the auspices of the U. S. Department of Energy, Office of Science, Office of Biological and Environmental Research by Pacific Northwest National Laboratory under contract DE-AC05-76RL01830. The Cloudnet project was funded by the European Union from Grant EVK2-2000-00065. The development of the

VARCLOUD retrieval was funded by NERC grant NE/C519697/1. Work at BNL was performed under the auspices of the U. S. Department of Energy, Office of Science, Office of Biological and Environmental Research by Brookhaven National Laboratory under contract DE-AC02-98CH10886. The contribution of Gerald G. Mace is performed under the support by DOE grant DE-FG0398ER62571.

Appendix A: Description of the symbols and abbreviations in Table 2.

PSD	Particle size distribution
Exponential PSD	$N(r) = N_0 \exp(-\lambda r)$
Log-normal PSD	$N(\ln r) = \frac{N}{\sigma\sqrt{2\pi}} \exp(-(\ln r - \ln r_0)^2 / 2\sigma^2)$
(modified) gamma PSD	$N(r) = N_0 \exp(\alpha)(\frac{r}{r_0}) \exp(-\frac{r\alpha}{r_0})$
Normalized PSD	$N(D_{eq})=N_0 * F(D_{eq}/D_m)$
$F(D_{eq}/D_m)$	Normalized PSD
N, N_0	Number concentration, number concentration intercept
N_0*	number concentration intercept proportional to IWC/D_m^4
r, r_0	radius, modal radius
λ, α	parameters
σ	Standard width of log-normal distribution
D_{eq}, D_m	'equivalent melted' diameter, volume weighted diameter
DISORT	Discrete ordinate radiative transfer model (Stamnes et al. 1988)
LBLRTM	Line-by-Line radiative transfer model (Clough et al. 1981, 1992)
MODTRAN3	Moderate resolution atmospheric transmission version3 (Berk et al. 1989)
δ-2 stream model	δ-2 stream radiative transfer model (Toon et al. 1989)
γ, μ_0	Cloud transmissivity ratio, cosine of solar zenith angle
T, P, I	Temperature, pressure, and spectral radiation

T_{cb}	Cloud base temperature
LWP, R	Liquid water path, rain rate
Z, Z_e	Radar reflectivity, water equivalent radar reflectivity
V_d, σ_d	Radar Doppler velocity, Doppler velocity spectral width
σ_{ext}	Lidar extinction coefficient
W_m, W_σ	Mean air vertical velocity, standard deviation of the vertical motion
F( )	A function of …
a, b	parameters
f_{ice}	Cloud ice fraction
Z_{liquid}, Z_{ice}	Radar reflectivity from liquid contribution, ice contribution;
LWC, IWC	Liquid water content, ice water content
$r_{e,}$ r_{e_layer}	Effective radius, layer average effective radius
τ	Optical depth
EPM	Empirical parameterization method
Optimal	Radiation matching optimal estimation method
Forward	Forward approach which theoretically derives the cloud properties with assumptions.

760

Appendix B: A summary of main feature for nine cloud products

A brief summary of the major features for the nine ground-based cloud retrieval products, which are MICROBASE, MACE, CLOUDNET, DENG, SHUPE_TURNER, WANG, COMBRET, RADON and VARCLOUD, is given in this appendix.

MICROBASE is the ARM Continuous Baseline Microphysical Retrieval [Dunn et al. 2011]. In principle, it is an empirical estimate rather than a physically based retrieval. The liquid water content (LWC), liquid effective radius (r_e), and ice water content (IWC) are estimated from the Z based parameterization equations [Liao and Sassen 1994; Frisch et al. 1995; Liu and Illingworth 2000]; and the ice r_e is parameterized as a function of cloud temperature (T) [Ivanova et al. 2001]. Note that the LWC in MICROBASE has been scaled by MWRRET LWP before it is used for the derivation of liquid r_e. A constant droplet number concentration of 200 cm^{-3} has been used for the retrieval of liquid r_e at all 5 sites. For mixed phase clouds with temperature range between -16 and 0 degree C, MICROBASE introduces an ice fraction $f_{ice} = -T/16$ based on the environmental temperature to separate the radar reflectivity contributed from ice and liquid particles and then retrieves the cloud liquid and ice properties from the corresponding radar reflectivity [Dunn et al. 2011]. Note that MICROBASE has assumed the liquid clouds with non-precipitation and no entrainment. The particular empirical relationships used in the MICROBASE algorithm were chosen based on a series of surface and top-of-atmosphere radiative closure exercises [Mlawer et al. 2008]. The MICROBASE algorithm is broadly applied to all cloud types and for all conditions.

MACE, in contrast to MICROBASE, uses more physically based retrieval techniques to derive the cloud properties for stratus and cirrus. In short, MACE derives the daytime stratus layer averaged liquid r_e using an optimal estimation method to converge the modeled cloud shortwave transmissivity ratio to that measured for optically thin clouds and a parameterization method for optically thick clouds [Dong et al. 1998]. It derives the profiles of stratus cloud properties by scaling the layer averaged r_e and MWRRET LWP with profiles of radar reflectivity [Dong and Mace 2003] and derives the cirrus cloud properties using an infrared radiance and radar reflectivity based optimal estimation technique [Mace et al. 1998] and a radar based forward approach [Mace et al. 2002]. For clouds that cannot be retrieved with the physically based retrieval algorithms mentioned above, like nighttime liquid clouds and ice clouds other than cirrus, MACE uses empirical radar relationships [Frisch et al. 1998; Liu and Illingworth 2000]. These algorithms as applied in the data used in this study are fully described and evaluated using radiative closure in Mace et al. (2006, 2008).

CLOUDNET retrieves LWC using a forward approach and IWC using a parameterization method. For LWC, CLOUDNET identifies the liquid cloud tops and bases in each profile, calculates the adiabatic liquid water content in each layer based on profiles of temperature and pressure from the European Centre for Medium-Range Weather Forecast (ECMWF), and then linearly scales these LWC values to yield the observed MWR LWP. The IWC parameterization equation used in CLOUDNET is a function of both radar reflectivity and cloud temperature, which makes IWC vary smoothly [Hogan et al. 2006a].

DENG provides ice only cloud properties using a physically based optimal estimation approach based on radar measurements of Z, V_d and σ_d [Deng and Mace 2006]. Similar as that used by MACE for cirrus clouds [Mace et al. 2002], the algorithm used by DENG also makes use of the dependence of the radar reflectivity, Doppler velocity, and Doppler spectral width on the particle size distribution. One unique feature in DENG is the treatment of the turbulence, which is considered as a parameter in the retrieval algorithm and predetermined from the Doppler spectrum width and radar reflectivity. For ice crystal habit, DENG assumes hexagonal columns instead of the bullet rosettes assumed by MACE.

SHUPE_TURNER derives cloud liquid r_e using AERI-based retrieval method for optical thin (optical depth<6) clouds [Turner 2005], a parameterization method [Frisch et al. 1995] for other liquid only clouds, and a value of 8 um for optical thick, multiphase cloud scenes that cannot be retrieved. A radar reflectivity based parameterization method [Frisch et al. 1995] is used to derive the LWC for liquid only clouds, in which the number concentration has been adjusted to make integrated LWC match MWRRET LWP. For clouds in which this parameterization method does not work, the LWC is derived using an adiabatic calculation scaled by the MWRRET LWP. For ice cloud properties, SHUPE_TURNER derives r_e using the AERI-based retrieval method for optical thin clouds and using the radar reflectivity based parameterization method [Shupe et al. 2005] for other clouds. IWC is obtained using a radar reflectivity based empirical parameterization method [Shupe et al. 2005].

WANG, similar to SHUPE_TURNER, also provides mixed-phase cloud properties at NSA. WANG considers the liquid and ice in mixed phase clouds as two separated layers and then obtains their properties [Wang et al. 2004]. It first obtains the cloud ice properties based on radar reflectivity (Z) and lidar extinction coefficient (σ_{ext}) using a forward approach [Wang and Sassen 2002] and then derives the cloud liquid r_e by converging the model calculated cloud infrared spectral radiance (ice effects considered based on ice properties) to the measured cloud spectral radiance [Wang et al. 2004]. The LWC in WANG follows an adiabatic profile estimated with cloud base and top height and cloud base temperature, and is further constrained with the derived MWR LWP by Wang (2007).

COMBRET obtains the cloud properties by combining several retrieval algorithms, which vary depending on the input measurements available. For cloud liquid properties, COMBRET uses the similar methods as MICROBASE for clouds detected by the radar, except that the number concentration is set to 100 cm^{-3} as the clouds at the tropical ARM sites are assumed to be more representative of maritime conditions. When radar measurements are not available, liquid r_e is set a value of 5 um and LWC is calculated from lidar σ_{ext} and assumed liquid r_e. For cloud ice properties, COMBRET uses both radar and lidar measurements, following the same method as WANG when both Z and σ_{ext} are available but using fitting parameterization methods when only Z or σ_{ext} is available, including the Z and T-based parameterization method used by CLOUDNET. Unlike MICROBASE, COMBRET classifies drizzle and rain from the liquid clouds and derives their properties using a radar reflectivity based parameterization method.

RADON provides ice only cloud properties based on measurements of radar reflectivity and Doppler velocity at TWPC3. The retrieval method has been described by Delanoë et al. (2007). The unique feature of RADON (and VARCLOUD) consists in scaling the particle size distribution [Delanoë et al. 2005], leaving two unknowns to be retrieved: the intercept parameter of the normalized particle size distribution (N_0^*) and the mean volume-weighted diameter (D_m). It first derives the vertical air velocity, ice particle terminal fall speed, and ice particle density-maximum diameter relationship based on the relationship between measured Doppler velocity and radar reflectivity. D_m is derived from particle terminal velocity V_t and N_0* from the combination of V_t and radar reflectivity. IWC and extinction (σ_{ext}) are calculated using N_0*, D_m and the normalized particle size distribution. Ice r_e is then calculated as proportional to the ratio of IWC to σ_{ext} as in Stephens et al. (1990).

VARCLOUD also provides ice only cloud properties at TWPC3 using a variational scheme developed by Delanoë and Hogan (2008). This algorithm retrieves ice cloud properties (visible extinction, IWC and effective radius) seamlessly between regions of the cloud detected by both radar and lidar, and regions detected by just one of these two instruments. The retrieval technique uses the optimal estimation framework to minimize iteratively the difference between the forward-modelled observations and real observations. It includes a rigorous treatment of measurements and forward model errors. At each step, forward-modeled radar reflectivity and lidar-attenuated backscatter are computed using the forward model and the state vector containing extinction, extinction-to-backscatter ratio and number concentration. Once the convergence is achieved, the optimal state vector is converted to IWC and ice r_e using look-up

tables. The forward model assumes a microphysical model describing the shape of the particle size distribution using the normalized approach [Delanoë et al. 2005]. The mass-size relationship, used to derive the look-up table linking ice cloud properties to measurements parameters, follows a power law proposed by Brown and Francis (1995) for spherical aggregates. The lidar forward model accounts for multiple scattering and attenuation using the model of Hogan (2006). Extinction-to-backscatter ratio is retrieved with a vertically constant assumption.

_____

Chuanfeng Zhao

LLNL, Mail Code L-103

7000 East Ave

Livermore, CA 94550

zhao6@llnl.gov

Reference:

Ackerman, T. P., and G. M. Stokes (2003), The Atmospheric Radiation Measurement Program, *Phys. Today*, **56**, 38–44.

Bailey, M., and J. Hallett (2009), A comprehensive habit diagram for atmospheric ice crystals: Confirmation from the laboratory, AIRS II, and other field studies, *J. Atmos. Sci.*, **66**, 2888-2899.

Berk, A., L. S. Bernstein, and D. C. Robertson (1989), *MODTRAN: A Moderate Resolution Model for LOWTRAN 7*, Technical Report GL-TR-89-0122, Geophys. Lab, Bedford, MA.

Brown, P. R. A., and P. N. Francis (1995), Improved measurements of the ice water content in cirrus using a total-water probe. *J. Atmos. Oceanic Technol.,* **12,** 410. 414.

Clough, S. A., F. X. Kneizys, L. S. Rothman, and W. O. Gallery (1981), Atmospheric spectral transmittance and radiance: FASCOD1B, *Proc. of Soc. Photo. Opt. Instrum. Eng.*, **277**, 152-166.

Clough, S. A., M. J. Iacono, and J. L. Moncet (1992), Line-by-line calculations of atmospheric fluxes and cooling rates: application to water vapor. *J. Geophys. Res.*, **97**, 15761-15785.

Comstock, J. M., and K. Sassen, 2001: Retrieval of cirrus cloud radiative and backscattering properties using combined lidar and infrared radiometer (LIRAD) measurements. *J. Atmos. Oceanic Technol.,* **18,** 1658–1673.

Comstock, Jennifer M., and Coauthors (2007), An Intercomparison of Microphysical Retrieval Algorithms for Upper-Tropospheric Ice Clouds, *Bull. Amer. Meteor. Soc.*, **88**, 191–204. doi: 10.1175/BAMS-88-2-191.

Delanoë,J.,A. Protat, J. Testud, D. Bouniol, A. J. Heymsfield, A. Bansemer, P.R.A. Brown, and R. M. Forbes (2005), Statistical properties of the normalized ice particle size distribution. *J. Geophys. Res.*, **110**, 10201, doi:10.1029/2004JD005405.

Delanoë, J., A. Protat, D. Bouniol, A. Heymsfield, A. Bansemer, and P. Brown (2007), The characterization of ice clouds properties from Doppler radar measurements, *J. Appl. Meteor. Climatol.*, **46**, 1682–1698.

Delanoë, J., and R. J. Hogan (2008), A variational scheme for retrieving ice cloud properties from combined radar, lidar, and infrared radiometer, *J. Geophys. Res.*, **113**, D07204, doi:10.1029/2007JD009000.

Deng, M., and G. Mace (2006), Cirrus microphysical properties and air motion statistics using cloud radar Doppler moments. Part I: Algorithm description, *J. Appl. Meteor. Climatol.*, **45,** 1690–1709.

Dong, X., T. P. Ackerman, and E. E. Clothiaux (1998), Parameterizations of microphysical and shortwave radiative properties of boundary layer stratus from ground-based measurements, *J. Geophys. Res.*, **103**, 31,681–31,693.

Dong X., and G.G. Mace (2003), Profiles of Low-level Stratus Cloud Microphysics Deduced from Ground-based Measurements, *J. Atmos and Oceanic Tech.*, **20**, 42-53.

Dong, X., P. Minnis, B. Xi, S. Sun-Mack, and Y. Chen (2008), Comparison of CERES-MODIS stratus cloud properties with ground-based measurements at the DOE ARM Southern Great Plains site, *J. Geophys. Res.*, **113**, D03204, doi:10.1029/2007JD008438.

Dunn, M., M. P. Jensen, K. Johnson, M. Miller, E. Clothiaux, G. Mace, R. Marchand, and J. Mather (2009), A status report and update on the microbase VAP. Atmospheric Radiation

Measurement (ARM) Program Science Team Meeting, Louisville, KY, March 30-April 3, 2009.

Dunn, M., R. J. Hogan, E. J. O'Connor, M. P. Jensen, and D. Huang (2010), A comparison of cloud microphysical quantities with forecasts from cloud prediction models. The First Science Team Meeting of the Atmospheric System Research (ASR) Program, Bethesda, MD, March 15-19, 2010.

Dunn, M., K. L. Johnson and M. P. Jensen (2011), The Microbase value-added product: A baseline retrieval of cloud microphysical properties. DOE/SC-ARM/TR-095. http://www.arm.gov/publications/tech_reports/doe-scp-arm-tr-095.pdf

Frisch, A. S., C. W. Fairall, and J. B. Snider (1995), Measurement of stratus cloud and drizzle parameters in ASTEX with K„ -band Doppler radar and amicrowave radiometer, *J Atmos. Sci.*, **52**, 2788-2799.

Frisch, A. S., G. Feingold, C. W. Fairall, T. Uttal, and J. B. Snider (1998), On cloud radar and microwave radiometer measurements of stratus cloud liquid-water profiles, *J. Geophys. Res.*, **103**, 23,195-23,197.

Fu, Q. (1996), An accurate parametrization of the solar radiative properties of cirrus clouds for climate models, *J. Clim.* **9,** 2058-2082.

Fu, Q., (2007), A new parameterization of an asymmetry factor of cirrus clouds for climate models. *J. Atmos. Sci.*, **64**, 4144-4154.

Gaussiat, N., R. J. Hogan, and A. J. Illingworth (2007), Accurate liquid water path retrieval from low-cost microwave radiometers using additional information from a lidar ceilometer and operational forecast models. *J. Atmos. Oceanic Technol.*, **24**, 1562-1575.

Heymsfield, A. J. and J. Iaquinta (2000), Cirrus crystal terminal velocities, *J. Atmos. Sci*., **57**, 916-938.

Heymsfield, A. J., S. Lewis, A. Bansemer, J. Iaquinta, L. M. Milosovich, M. Kajikawa, C. Twohy, and M. R. Poellot (2002), A general approach for deriving the properties of cirrus and stratiform ice cloud particles, *J. Atmos. Sci.*, **59,** 3–29.

Heymsfield, A. J., S. Matrosov, and B. Baum (2003), Ice Water Path–Optical Depth Relationships for Cirrus and Deep Stratiform Ice Cloud Layers, *J. Appl. Meteor.*, **42**, 1369–1390.

Heymsfield, A. J., C. G. Schmitt, A. Bansemer, D. Baumgardner, E. M. Weinstock, J. T. Smith, and D. Sayres (2004), Effective ice particle densities for cold anvil cirrus, *Geophys. Res. Lett.*, **31**, doi:10.1029/2003GL018311.

Hobbs, P. V., A. L. Rangno, M. D. Shupe, and T. Uttal (2001), Airborne studies of cloud structures over the Arctic Ocean and comparisons with deductions from ship-based 35-GHz radar measurements, *J. Geophys. Res.*, **106**, 15,029-15,044.

Hogan, R. J., **(**2006), Fast approximate calculation of multiply scattered lidar returns. *Appl. Optics,* **45,** 5984–5992.

Hogan, R. J., M. P. Mittermaier, and A. J. Illingworth (2006a), The retrieval of ice water content from reflectivity factor and temperature and its use in evaluating a mesoscale model, *J. Appl. Meteor. Climatol.*, **45**, 301–317.

Hogan, R. J.**,** D. P. Donovan, C. Tinel, M. A. Brooks, A. J. Illingworth and J. P. V. Poiares Baptista (2006b), Independent evaluation of the ability of spaceborne radar and lidar to retrieve the microphysical and radiative properties of ice clouds. *J. Atmos. Oceanic Technol.*, **23,** 211–227.

Huang, D., K. Johnson, Y. Liu, and W. Wiscombe (2009), High resolution retrieval of liquid water vertical distributions using collocated Ka-band and W-band cloud radars, *Geophys. Res. Lett.*, **36**, L24807, doi:10.1029/2009GL041364.

Huang, D., C. Zhao, M. Dunn, X. Dong, G. G. Mace, M. Jensen, S. Xie, and Y. Liu (2011), An intercomparison of radar-based liquid cloud microphysics retrievals and implication for model evaluation studies, in preparation.

Illingworth, A. J., and Coauthors (2007), Cloudnet - continuous evaluation of cloud profiles in seven operational models using ground-based observations, *Bull. Am. Meteorol. Soc.*, **88**, 883-898.

IPCC Fourth Assessment Report: Climate Change 2007 (AR4).

Ivanova, D. C., D. L. Mitchell, W. P. Arnott, and M. Poellot (2001) A GCM parameterization for bimodal size spectra and ice mass removal rates in mid-latitude cirrus clouds, *Atmos. Res.*, **59**, 89-113.

Klein, S. A., and coauthors (2009), Intercomparison of model simulations of mixed-phase clouds observed during the ARM Mixed-Phase Arctic Cloud Experiment. I: single-layer cloud, *Q. J. R. Meteorol. Soc.*, **135**, 979–1002. doi: 10.1002/qj.416

Korolev, A., G. A. Isaac, and J. Hallett (1999), Ice particle habits in Arctic clouds, *Geophys. Res. Lett.*, **26**, 1299–1302.

Kubar, T. L., D. L. Hartmann, and R. Wood (2009), Understanding the Importance of Microphysics and Macrophysics for Warm Rain in Marine Low Clouds. Part I: Satellite Observations. *J. Atmos. Sci.*, **66**, 2953–2972. doi: 10.1175/2009JAS3071.1

Liao, L., and K. Sassen (1994), Investigation of relationships between Ka-band radar reflectivity and ice and liquid water contents, *Atmos. Res.*, **34**, 231-248.

Lin, B., P. Minnis, and A. Fan (2003), Cloud liquid water path variations with temperature observed during the Surface Heat Budget of the Arctic Ocean (SHEBA) experiment, *J. Geophys. Res.*, **108,** 4427, doi:10.1029/2002JD002851.

Liu, C.-L., and A. J. Illingworth (2000), Towards more accurate retrievals of ice water content from radar measurement of clouds, *J. Appl. Meteorol.*, **39,** 1130-1146.

Mace, G. G., T. P. Ackerman, P. Minnis, and D. F. Young (1998) Cirrus layer microphysical properties derived from surface-based millimeter radar and infrared interferometer data, *J. Geophys. Res.*, **103**, 23,207-23,216.

Mace, G. G., A. J. Heymsfield, and M. R. Poellot (2002), On retrieving the microphysical properties of cirrus clouds using the moments of the millimeter wavelength Doppler spectrum, *J. Geophys. Res.*, **107**, 4815-4841.

Mace, G. G., S. Benson, K. Sonntag, S. Kato, Q. Min, P. Minnis, C. Twohy, M. Poellot, X. Dong, C. Long, Q. Zhang, and D. Doelling (2006), Cloud radiative forcing at the ARM climate research facility: Part 1. technique, validation, and comparison to satellite-derived diagnostic quantities. *J. Geophys. Res.*, **111**, D11S90, doi:10.1029/2005JD005921.

Mace, G. G., and S. Benson (2008), The vertical distribution of cloud radiative forcing at the SGP ARM Climate Research Facility as revealed by 8-years of continuous data, *J. Climate*, **21**, 2591-2610.

MacFarlane, S. A., K. F. Evans, and A. S. Ackerman (2002), A Bayesian algorithm for the retrieval of liquid water cloud properties from microwave radiometer and millimeter radar data. *J. Geophys. Res.*, **107**, D16, 4317, doi:10.1029/2001JD001011.McFarlane, S. A. and R. T. Marchand (2008), Analysis of ice crystal habits derived from MISR and

MODIS observations over the ARM Southern Great Plains site, *J. Geophys. Res.*, 113, D07209, doi:10.1029/2007JD009191.

McFarquhar, G. M., and A. J. Heymsfield (1996), Microphysical characteristics of three anvils sampled during the Central Equatorial Pacific Experiment (CEPEX), *J. Atmos. Sci.*, **53**, 2401-2423.

McFarquhar, G. M., and A. J. Heymsfield (1998), The definition and significance of an effective radius for ice clouds, *J. Atmos. Sci.*, **55**, 2039-2052.

McFarquhar, G. M., G. Zhang, M. R. Poellot, G. L. Kok, R. McCoy, T. Tooman, A. Fridlind, and A. J. Heymsfield (2007), Ice properties of single-layer stratocumulus during the Mixed-Phase Arctic Cloud Experiment: 1. Observations, *J. Geophys. Res.*, **112**, D24201, doi:10.1029/2007JD008633.

Mitchell, D. L., S. K. Chai, Y. Liu, A. J. Heymsfield, and Y. Dong (1996), Modeling cirrus clouds. Part I: Treatment of bimodal size spectra and case study analysis, *J. Atmos. Sci.*, **53,** 2952–2966.

Mlawer, E., and Coauthors (2008), Evaluating cloud retrieval algorithms with the ARM BBHRP framework. Eighteenth Annual Atmospheric Radiation Measurement (ARM) Science Team Meeting, Norfolk, VA, March 10-14, 2008.

Moran, K. P., B. E. Martner, M. J. Post, R. A. Kropfli, D. C. Welsh and K. B. Widener (1998), An unattended cloud-profiling radar for use in climate research. *Bull. Amer. Meteor. Soc.*, **79**, 443 -455.

Noel, V., D. M. Winker, M. McGill, and P. Lawson (2004), Classification of particle shapes from lidar depolarization ratio in con- vective ice clouds compared to in situ observations during CRYSTAL-FACE, *J. Geophys. Res.*, **109,** D24213, doi:10.1029/2004JD004883.

Noel, V., H. Chepfer, M. Haeffelin, and Y. Morille (2006), Classification of ice crystal shapes in midlatitude ice clouds from three years of lidar observations over the SIRTA observatory, *J. Atmos. Sci.*, **63**, 2978-2991.

Platt, C. M. R., S. A. Young, and J. H. Churnside (1998), The optical properties of equatorial cirrus from observations in the ARM Pilot Radiation Observation Experiment, *J. Atmos. Sci.*, **55**, 1977-1996.

Protat, A., G. M. McFarquhar, J. Um, J. Delanoë (2011), Obtaining best estimates for the microphysical and radiative properties of tropical ice clouds from TWP-ICE in situ microphysical observations, *J. Appl. Meteor. Climatol.*, **50**, 895–915. doi: 10.1175/2010JAMC2401.1.

Ramanathan, V., E. F. Harrison and B. R. Barkstrom, (1989), Cloud-Radiative Forcing and Climate: Results from the Earth Radiation Budget Experiment, *Science* **243** (4887), 57-63. doi:10.1126/science.243.4887.57.

Ramanathan, V. (1987), Atmospheric General Circulation and Its Low Frequency Variance: Radiative Influences, *J. Meteorol. Soc. of Japan*, Special Volume: 1512-1576.

Rossow, W. B., and R. A. Schiffer (1999), Advances in understanding clouds from ISCCP, *Bull. Amer. Meteorol. Soc.*, **80**, 2261-2288, doi:10.1175/1520-0477.

Schwartz, C., and G. G. Mace (2011), More analysis of cirrus cloud particle size distributions measured during SPARTICUS, The second annual ASR Science Team Meeting, San Antonio, TX, March 27-April 1, 2011.

Shupe, M.D., and J.M. Intrieri (2004), Cloud radiative forcing of the Arctic surface: The influence of cloud properties, surface albedo, and solar zenith angle, *J. Climate*, **17**, 616-628.

Shupe, M. D., P. Kollias, S. Y. Matrosov, and T. L. Schneider (2004), Deriving mixed-phase cloud properties from Doppler radar spectra, *J. Atmos. Oceanic Technol.,* **21,** 660–670.

Shupe, M., T. Uttal, and S. Y. Matrosov (2005), Arctic Cloud Microphysics Retrievals from Surface-Based Remote Sensors at SHEBA, *J. Appl. Meteor.*, **44**, 1544–1562.

Shupe, M. D. (2007), A ground-based multi sensor cloud phase classifier, *Geophys. Res. Lett.*, **34**, L22809, doi:10.1029/2007GL031008.

Shupe M. D., and Coauthors (2008), A focus on mixed-phase clouds: The status of ground-based observational methods, *Bull. Amer. Meteor. Soc.*, **89,** 1549–1562.

Shupe, M. D. (2011), Clouds at Arctic Atmospheric Observatories, Part II: Thermodynamic phase characteristics. *J. Appl. Meteor. Clim.*, **50**, 645-661.

Stamnes, K., S. C. Tsay,W.Wiscombe, and K. Jayaweera (1988), A numerically stable algorithm for discrete-ordinate-method radiative transfer in multiple scattering and emitting layered media, *Appl. Opt.*, **27**, 2502-2509.

Stephens, G. L., Tsay, Si-Chee, P. W. Stackhouse, and P. J. Flateau (1990), The relevance of the microphysical and radiative properties of cirrus clouds to climate and climate feedback, *J. Atmos. Sci*., **47**, 1742-1753.

Taylor, K. E. (2001), Summarizing multiple aspects of model performance in a single diagram, *J. Geophys. Res.*, **106**, 7183–7192, doi:10.1029/2000JD900719.

Toon, O. B., C. P. McKay, T. P. Ackerman, and K. Santhanam (1989), Rapid calculation of radiative heating rates and photodissociation rates in inhomogeneous multiple scattering atmospheres, *J. Geophys. Res.*, **94**, 16287-16301.

Turner, D. D. (2005), Arctic mixed-phase cloud properties from AERI-lidar observations: Algorithm and results from SHEBA, *J. Appl. Meteor.*, **44,** 427–444.

Turner, D. D. (2007), Improved ground-based liquid water path retrievals using a combined infrared and microwave approach, *J. Geophys. Res.*, **112**, D15204, doi:10.1029/2007JD008530.

Turner D. D., and coauthors (2007a), Thin liquid water clouds: Their importance and our challenge, *Bull. Amer. Meteor. Soc.*, **88**, 177-190.

Turner, D. D., S. A. Clough, J. C. Liljegren, E. E. Clothiaux, K. Cady-Pereira, and K. L. Gaustad (2007b), Retrieving liquid water path and precipitable water vapor from Atmospheric Radiation Measurement (ARM) microwave radiometers, *IEEE Trans. Geosci. Remote Sens.*, **45**(11), 3680–3690.

Verlinde, J., and Coauthors (2007), The Mixed-Phase Arctic Cloud Experiment, *Bull. Amer. Meteor. Soc.*, **88**, 205-221.

Wang, Z., and K. Sassen (2002), Cirrus cloud microphysical property retrieval using lidar and radar measurements: I algorithm description and comparison with in situ data, *J. Appl. Meteor.*, **41**, 218-229.

Wang, Z., K. Sassen, D.N. Whiteman, and B.B. Demoz (2004), Studying Altocumulus with Ice Virga Using Ground-Based Active and Passive Remote Sensors, *J. Appl. Meteor.*, **43**, 449-460.

Wang, Z., Q. Miao, and M. Zhao (2007), A Long-term Cloud Microphysical Properties Dataset for Arctic Cloud Study Based on ACRF NSA Site Observations. *Proceedings of the Seventeenth ARM Science Team Meeting*, March 26 to 30, 2007, Monterey, California.

Wang, Z. (2007), A refined two-channel microwave radiometer liquid water path retrieval for cold regions by using multiple-sensor measurements, *IEEE Geoscience & remote sensing letters*, **4**, 591-595.

Wylie, D. P., D. L. Jackson, W. P. Menzel, and J. J. Bates (2005), Trends in global cloud cover in two decades of HIRS observations. *J. Climate*, **18,** 3021–3031.

Xie, S., and Coauthors, (2005), Simulations of midlatitude frontal clouds by SCMs and CSRMs during the ARM March 2000 Cloud IOP. *J. Geophys. Res.*, **110**, D15S03, doi:10.1029/2004JD005119.

Xie, S., and coauthors (2010), CLOUDS AND MORE: ARM Climate Modeling Best Estimate Data, *Bull. Amer. Meteor. Soc.*, **91**, 13–20.

Xu, K-M., and Coauthors, (2005), Modeling springtime shallow frontal clouds with cloud-resolving and single-column models. *J. Geophys. Res.*, **110**, D15S04, 10.1029/2004JD005153.

Yost, C. R., P. Minnis, J. K. Ayers, R. Palikonda, D. Spangenberg, F. L. Change, S. Sun-Mack, P. W. Heck, and R. P. Lawson (2011), Evaluation of in-situ and satellite-derived cirrus microphysical properties during SPARTICUS. The Second Science Team Meeting of the Atmospheric System Research (ASR) Program, San Antonio, TX, March 28-April 1, 2011.

Zhao, C., and Coauthors (2011), Cloud Retrieval Ensemble Dataset (CRED), technical report, http://www-pcmdi.llnl.gov/ARM/cred/credreport.pdf.

Zhao, Y., G. G. Mace, and J. M. Comstock (2011), The occurrence of particle size distribution bimodality in midlatitude cirrus as inferred from ground-based remote sensing data. *J. Atmos. Sci.*, **68**, 1162–1177. doi: 10.1175/2010JAS3354.1

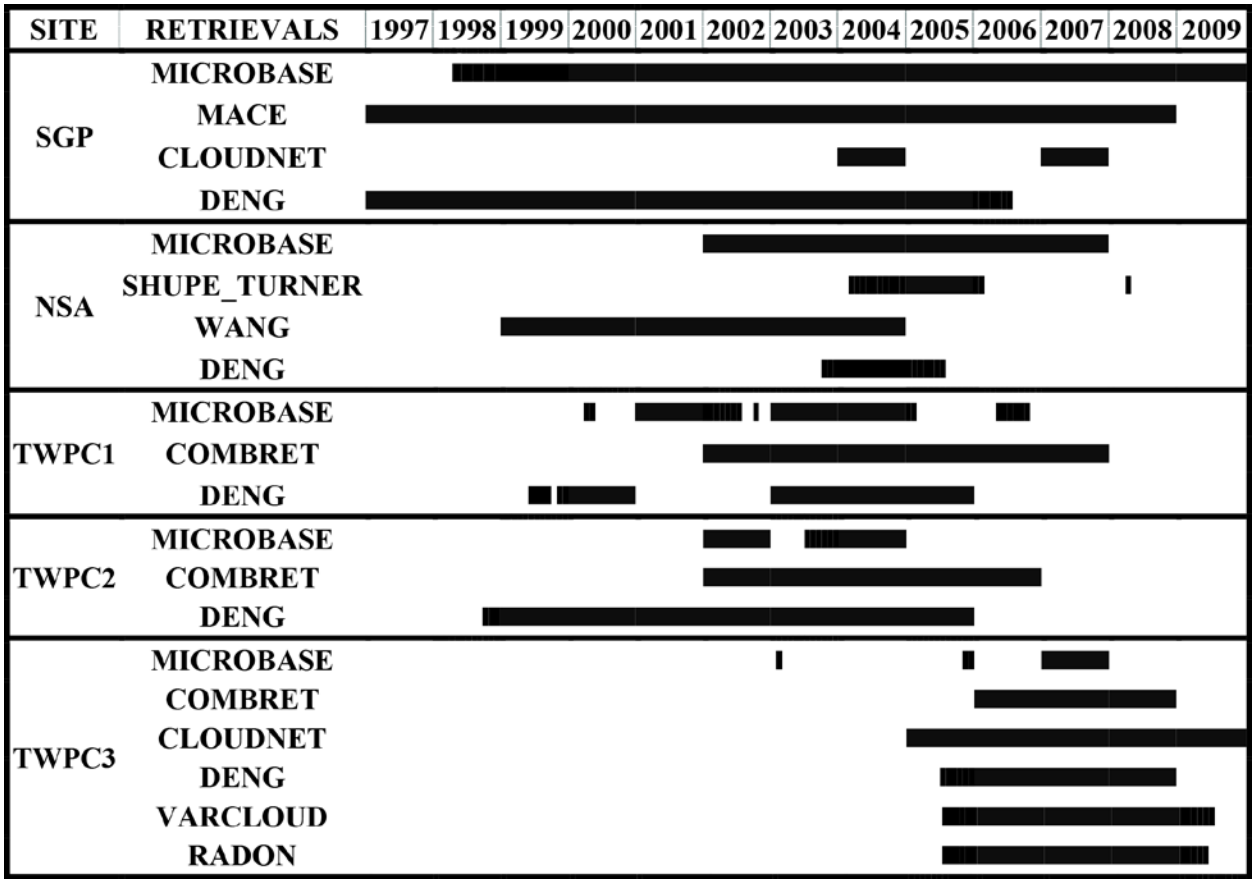

Figure1. Data availability for the nine ground-based cloud retrieval products between 1997 and 2009 at five permanent ARM research sites. MICROBASE, MACE, SHUPE_TURNER and COMBRET are for all cloud properties; CLOUDNET is for LWC and IWC of all clouds; DENG, VARCLOUD and RADON are for ice cloud properties only; and WANG is for mixed-phase cloud properties only.

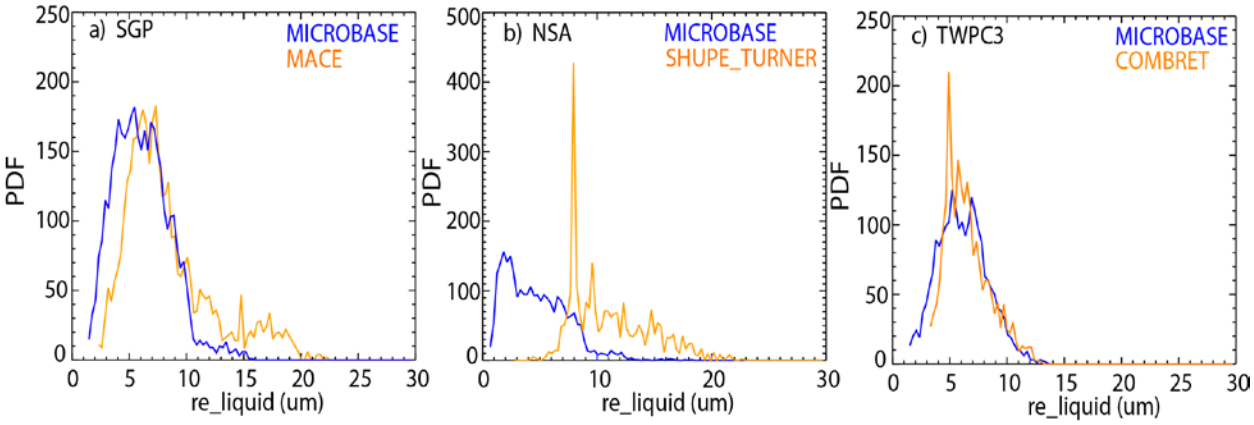

Figure 2. The retrieval difference of liquid r_e for exactly the same boundary single layer overcast clouds during the period of May through November for a) MICROBASE and MACE in 2004 at SGP, b) MICROBASE and SHUPE_TURNER in 2004 at NSA, and c) MICROBASE and COMBRET in 2007 at TWPC3.

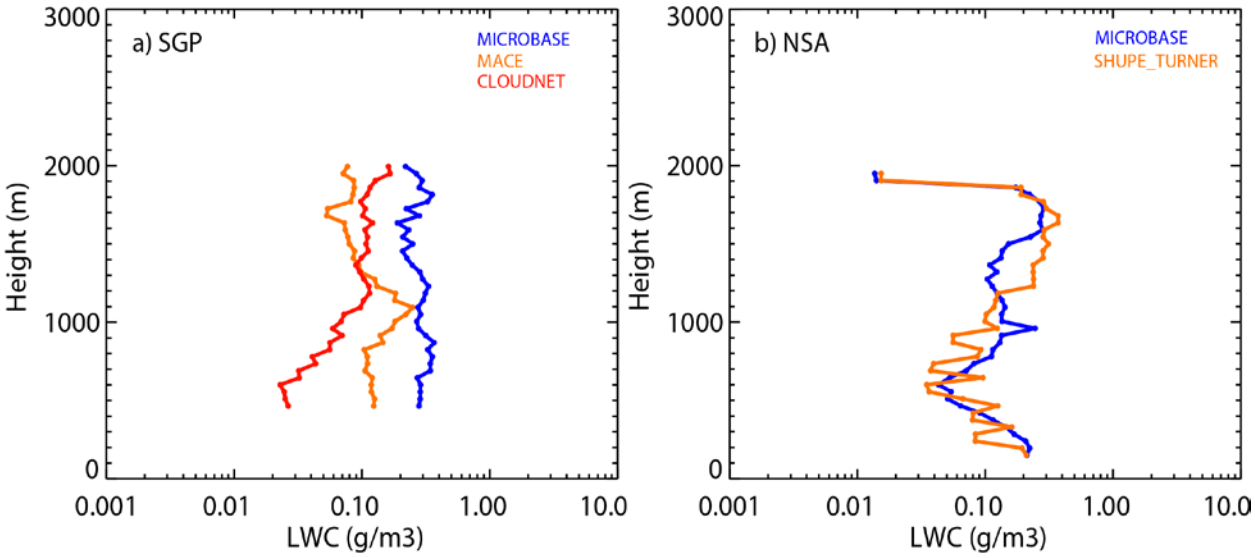

Figure 3. The differences of vertical distributions of mean LWC at each height for the same boundary single layer overcast clouds (liquid phase) from May through November in 2004 (a) between MICROBASE, MACE and CLOUDNET at SGP, and (b) between MICROBASE and SHUPE_TURNER at NSA.

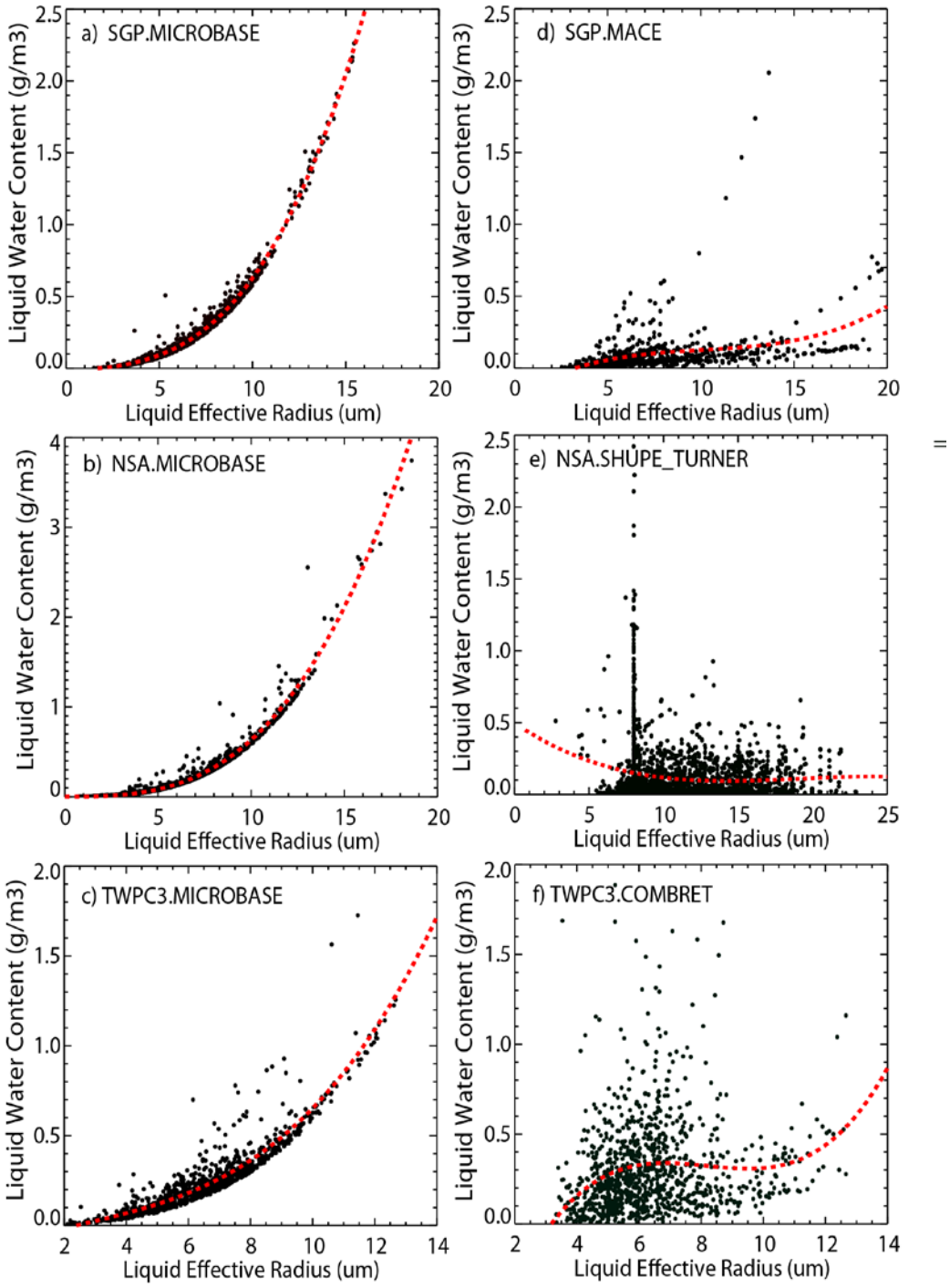

Figure 4. The relationship between LWC and liquid r_e for different retrieval products of pure liquid clouds during the period of May through November in 2004 at SGP and NSA, and in 2007 at TWPC3. The red lines are the fitting lines with a 2nd order polynomial function.

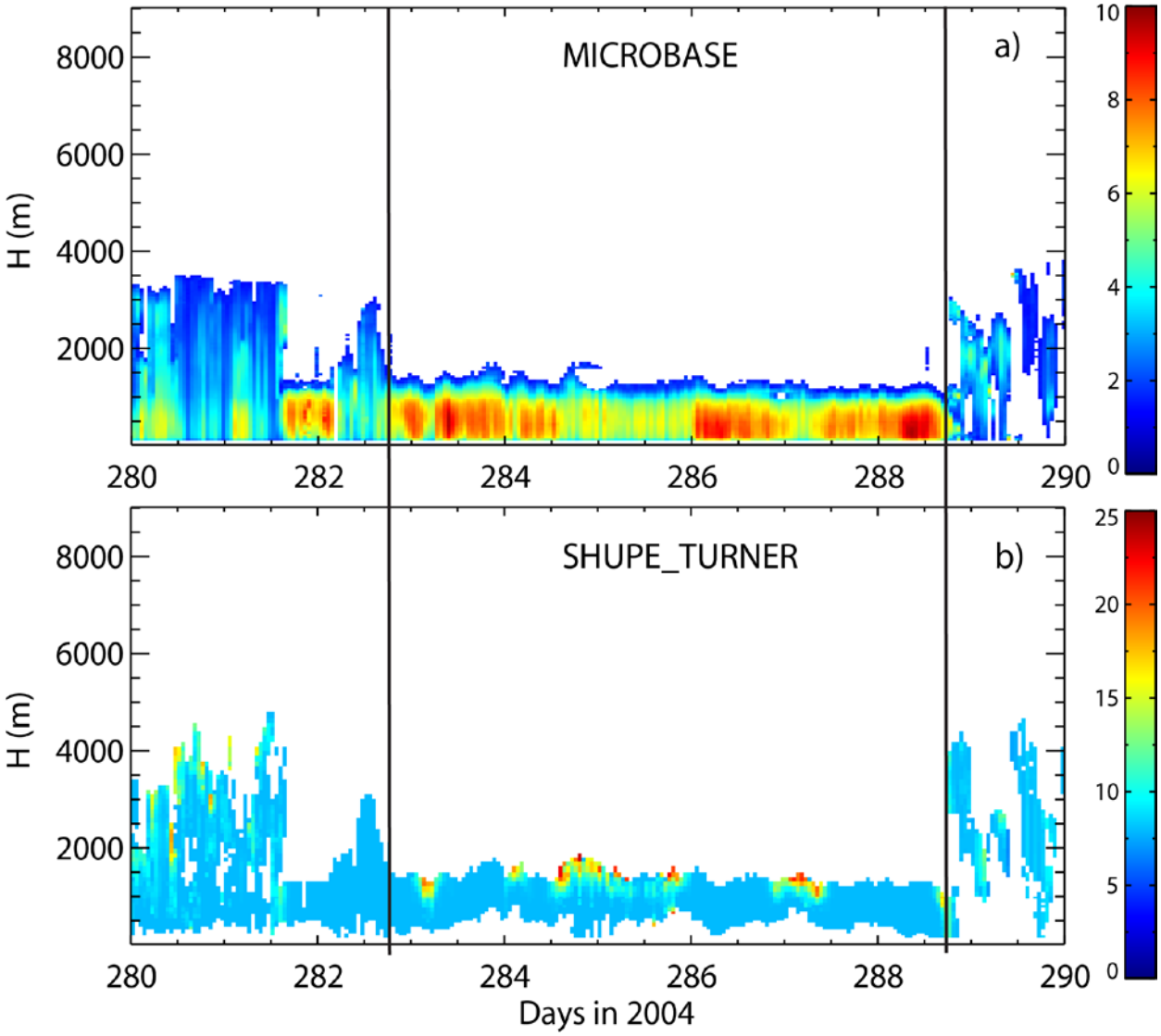

Figure 5. Difference in vertical structure of liquid r_e between (a) MICROBASE and (b) SHUPE_TURNER in October 2004 at NSA site.

1165

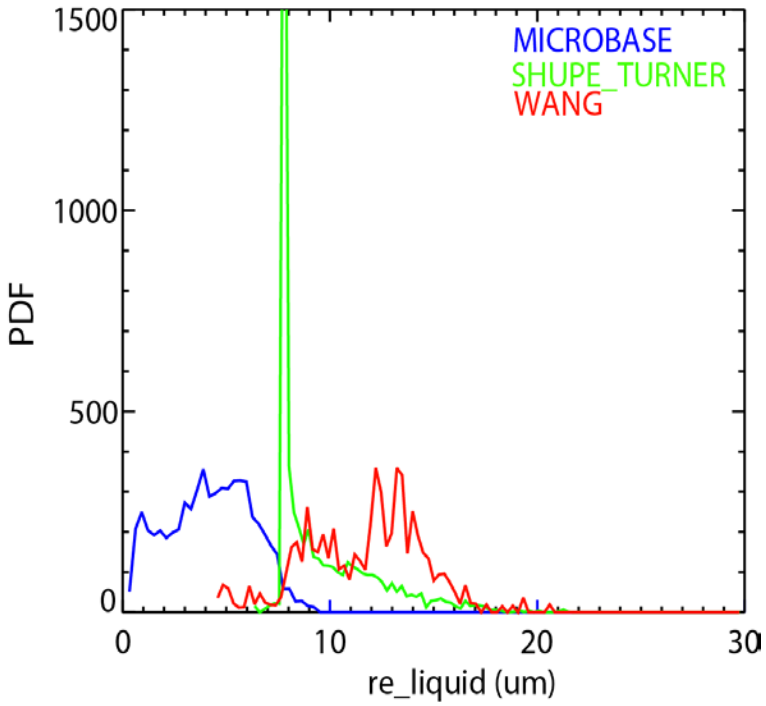

Figure 6. The difference in the cloud liquid r_e for the same single-layer, mixed-phase boundary layer clouds between retrievals from MICROBASE, SHUPE_TURNER, and WANG in May through November 2004 at NSA.

1170

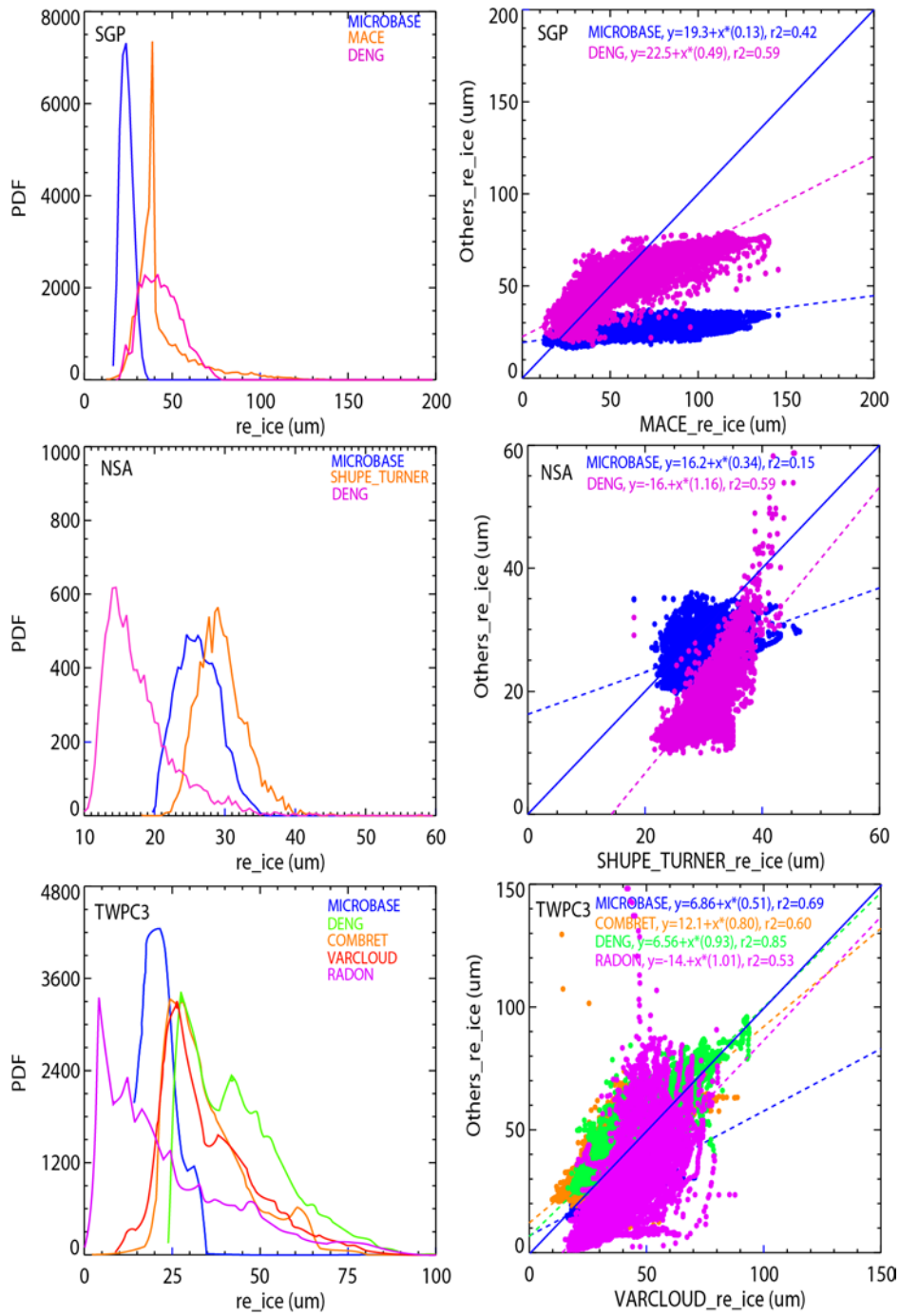

Figure 7. Differences in retrieved ice r_e between the ground-based retrieval products for high level ice clouds during the period between May and November in 2004 at SGP and NSA, and in 2007 at TWPC3.

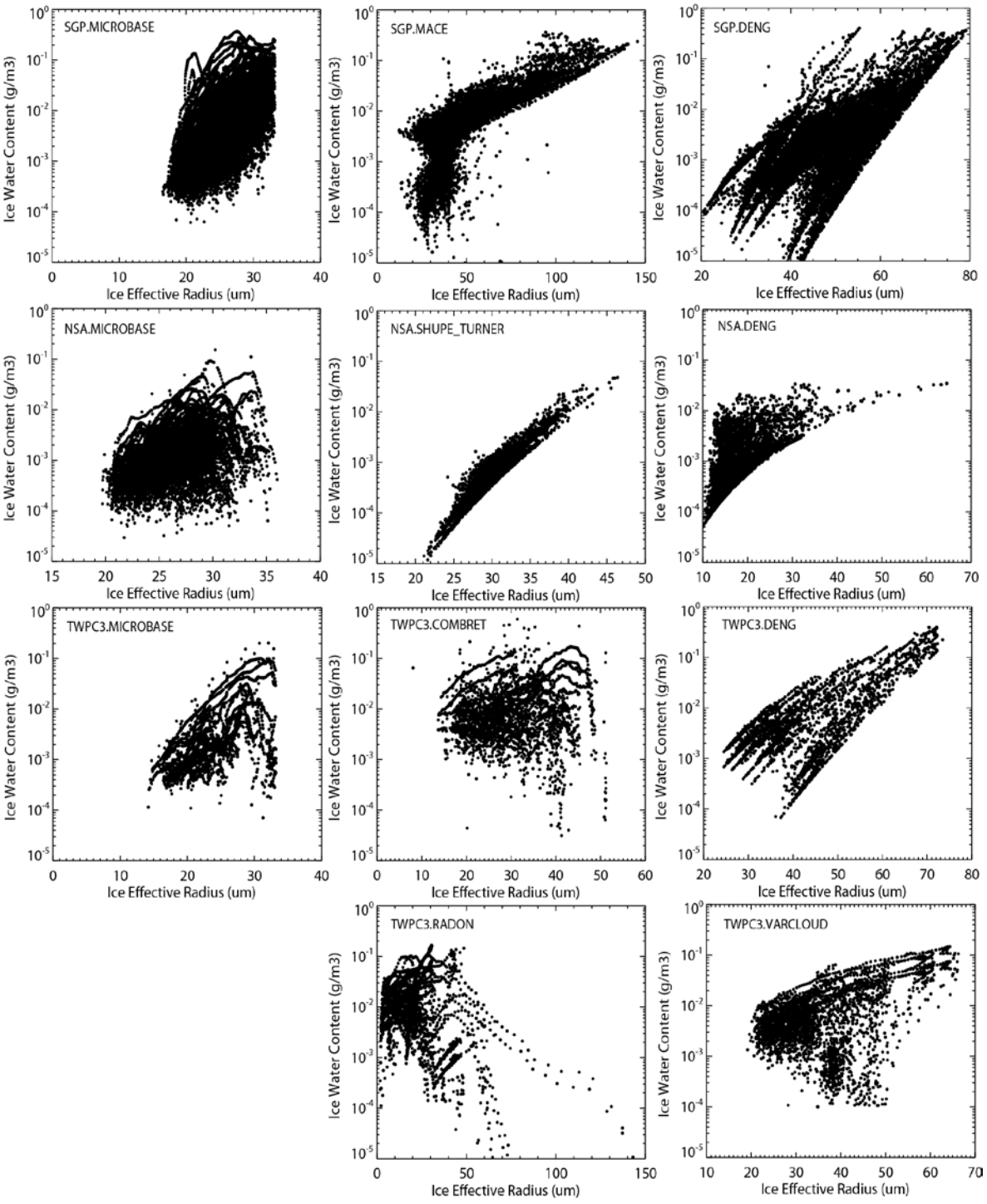

1175

Figure 8. Relationships between IWC and ice r_e for high level ice clouds between different retrievals for period of May through November in 2004 at SGP and NSA and in 2007 at TWPC3.

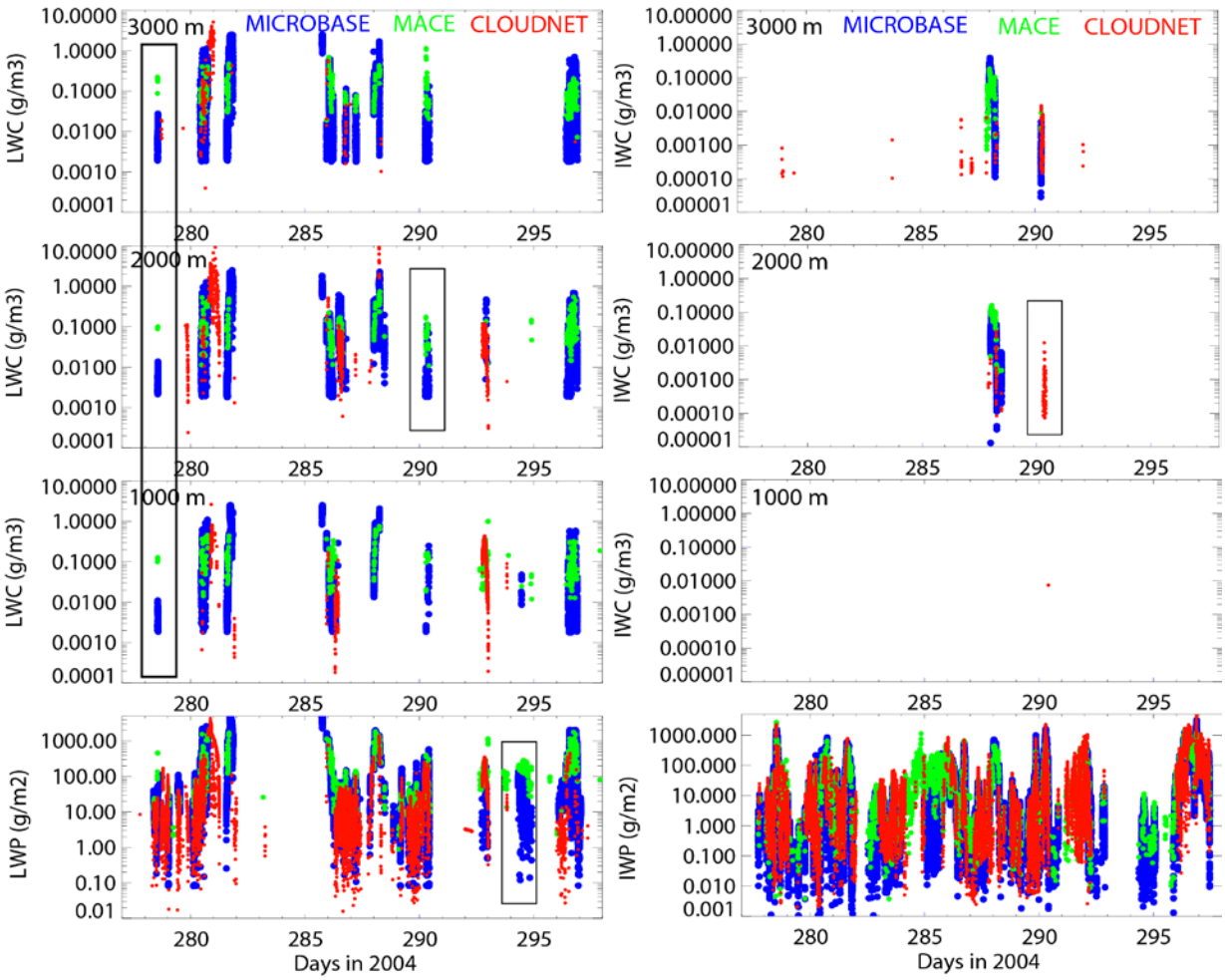

1180 Figure 9. The column integrated cloud liquid water path (LWP) and ice water path (IWP) along with cloud liquid water content (LWC) and ice water content (IWC) at heights of 1000 m, 2000 m, and 3000 m in October 2004 at SGP.

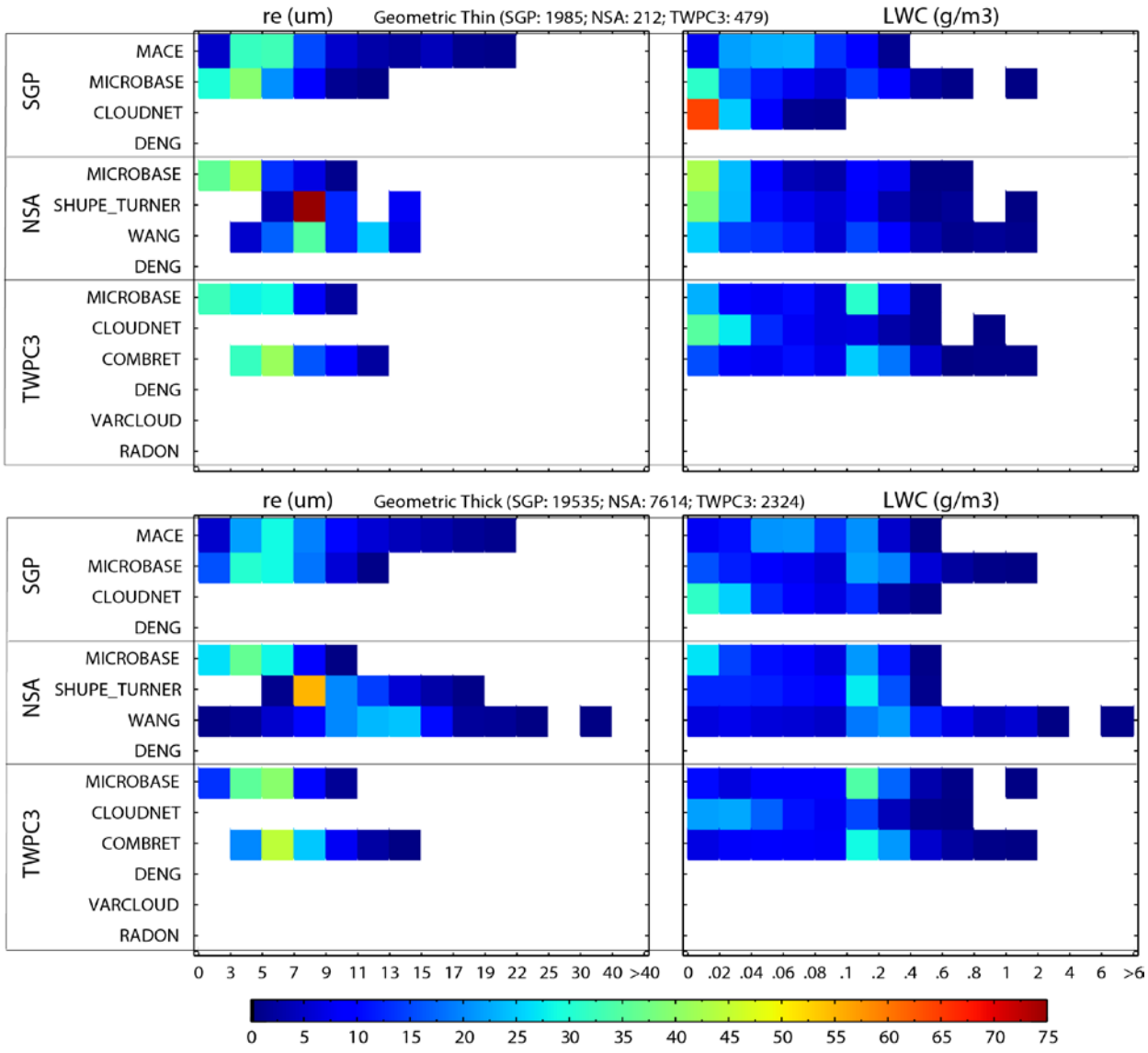

1185

Figure 10. Statistical distribution of cloud liquid r_e and LWC for geometric thin ($\Delta H \leq 300$ m) and geometric thick ($\Delta H > 300$ m) boundary layer overcast clouds. The numbers in the title are the total cloud samples used for this statistical analysis at each site.

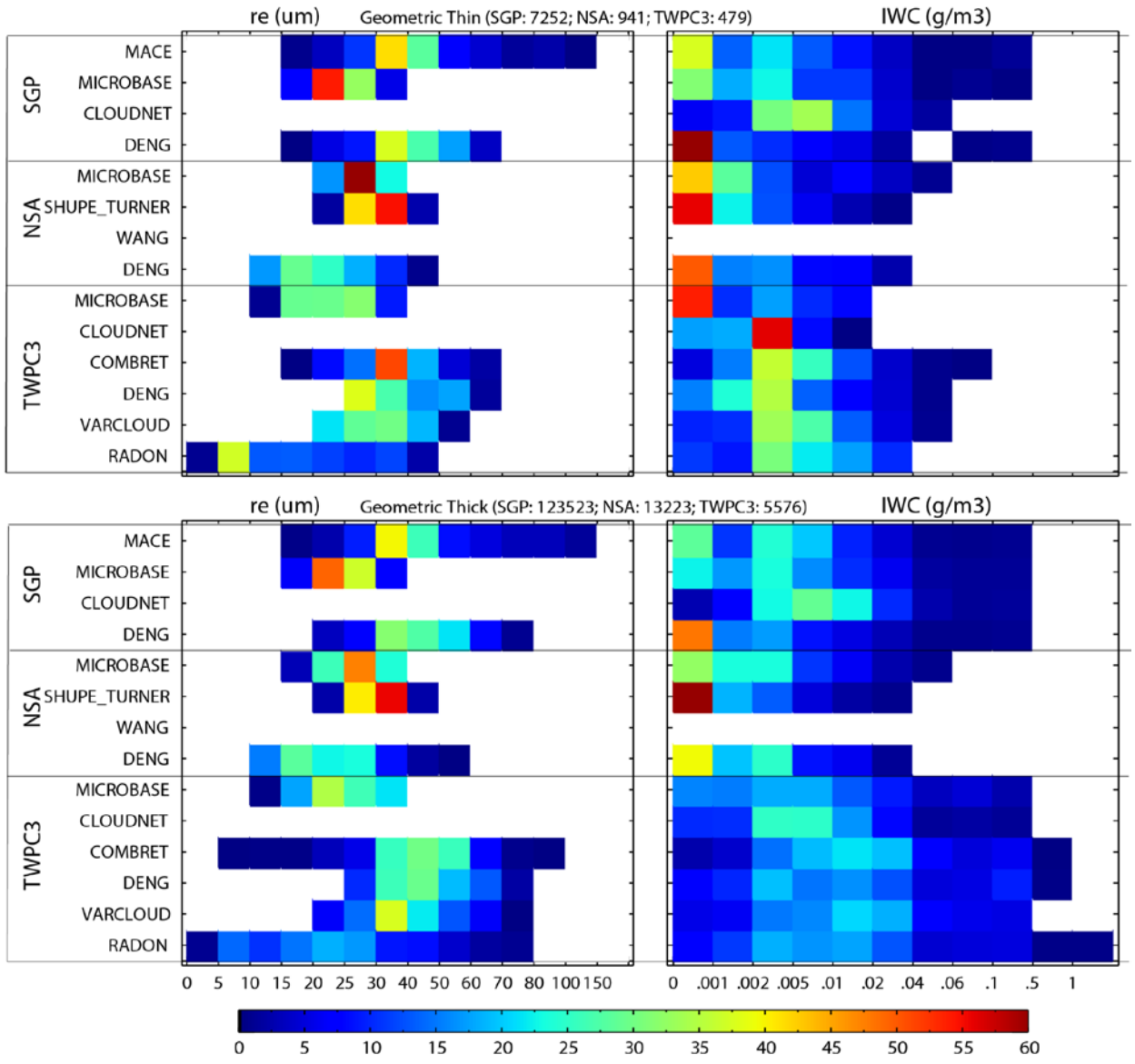

Figure 11. Statistical distribution of cloud ice r_e and IWC for geometric thin ($\Delta H \leq 600$ m) and geometric thick ($\Delta H > 600$ m) high level ice clouds. The numbers in the title are the total cloud samples used for this statistical analysis at each site.

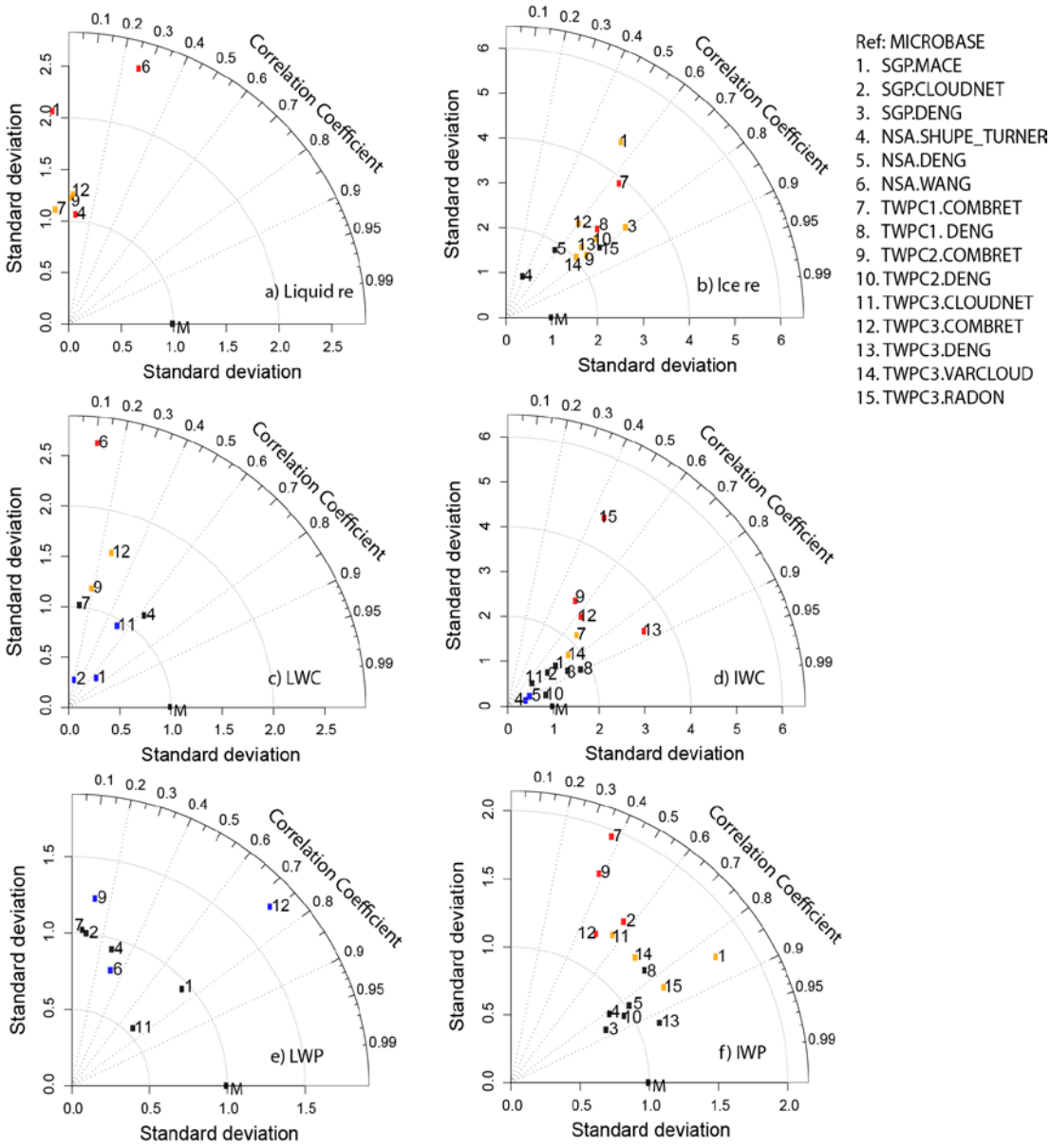

Figure 12. Taylor diagrams show the statistical correlation coefficients, relative standard deviation and centered root-mean-square errors for all retrieval products relative to MICROBASE regarding a) liquid r_e, b) ice re, c) LWC, d) IWC, e) LWP, f) IWP. The numbers in the plots indicate the different cloud retrieval products. The blue, black, yellow and red points indicate the ratio of mean values of the cloud properties from cloud products compared to MICROBASE are <0.7, 0.7-1.4, 1.4-2 and 2-4, respectively.

Table 1. Nine ground-based cloud retrieval products at 5 ARM sites along with their PI contact information and references.

Products	Contact PIs	Affiliations	Sites	Clouds	References
MICROBASE	Mike Jensen; Maureen Dunn	Brookhaven National Lab	All 5 sites	Liquid	Liao and Sassen 1994; Frisch et al. 1995
				Ice	Liu & Illingworth 2000; Ivanova et al. 2001
				Mixed	All above
MACE	Gerald Mace	University of Utah	SGP	Boundary Stratus	Dong et al. 1998 (Layer); Dong & Mace 2003(Profile)
				Other Liquid	Frisch et al. 1998
				Cirrus	Mace et al. 1998 (Layer Average); Mace et al. 2002 (Vertical Profile)
				Other Ice	Liu and Illingworth 2000
CLOUDNET	Robin Hogan; Ewan O'Connor	University of Reading	SGP, TWPC3	Liquid part	Illingworth et al. 2007
				Ice part	Hogan et al. 2006a
DENG	Min Deng	University of Wyoming	All 5 sites	Cirrus	Deng and Mace 2006
SHUPE_ TURNER	Matthew Shupe; David Turner	University of Colorado, NOAA National Severe Storms Lab	NSA	Liquid only	Frisch et al. 1995; Turner et al. 2007b; Turner 2007
				Liquid and ice in thin clouds	Turner 2005, 2007; Turner et al. 2007b
				Ice part	Shupe et al. 2005
WANG	Zhien Wang	University of Wyoming	NSA	Mixed	Wang and Sassen 2002 Wang et al. 2004; Wang et al. 2007
COMBRET	Jenifer Comstock	Pacific Northwest National Lab	3 TWP sites	Liquid (radar)	Same as MICROBASE
				Ice (radar+lidar)	Wang and Sassen 2002
				Ice (radar only)	Hogan et al. 2006a
				Ice (lidar only)	Comstock and Sassen 2001; Fu 2007
				Drizzle, rain	Wood 2005
RADON	Alain Protat; Julien Delanoë	CAWCR, LATMOS	TWPC3	Ice	Delanoë et al. 2007
VARCLOUD	Alain Protat; Julien Delanoë	CAWCR, LATMOS	TWPC3	Ice	Delanoë and Hogan 2008

CAWCR indicates 'the Centre for Australian Weather and Climate Research'; and LATMOS indicates 'the Laboratoire ATmosphère, Milieux, Observations Spatiales'.

Table 2 Retrieval algorithms (assumptions, retrieval ideas, functions and inputs) for nine cloud products. The meanings of the symbols and abbreviations are listed in the appendix.

Products	Clouds	Assumptions		Theory Based Functions/Models/parameters	Major Inputs	Method
		PSD	Habit			
MICROBASE	Liquid	Log-normal (σ=0.35)	spherical	LWC=F(Z, LWP); re=F(Z, LWC); N~200 cm^{-3}	Z	EPM
	Ice	Exponential	Planar polycrystal	IWC=F(Z_e); re=F(T)	Z_e, T	EPM
	Mixed	See above	See above	f_{ice}=-T/16; $Z_{liquid}=(1-f_{ice})*Z$; $Z_{ice}=f_{ice}*Z$	Z, T	EPM
MACE	Boundary stratus (layer)	log-normal (σ=0.35)	Spherical	Thick: r_{e_layer}=F(LWP, γ, μ0); Thin: δ-2 stream model	LWP, γ, μ0	EPM; optimal
	Boundary stratus (profile)	Log-normal	Spherical	LWC=F(LWP, Z); day: r_e=F($r_{e\ layer}$, Z); night: r_e=F(Z)	LWP, Z	Forward
	Other Liquid	-	spherical	LWC=F(LWP, Z); $<r^6>=<r^3>^2$	LWP, Z	Forward
	Cirrus (layer)	Modified Gamma (α=1)	hexagonal	MODTRAN3 model (optical thin)	Z_e, I	Optimal
	Cirrus (Profile)	Exponential	Bullet Rosette	Z_e=F(L, n(L)); V_d=F(L, n(L), V(L)); σ_d^2=F(L, n(L), V(L))	Z_e, V_d	Forward
	Other Ice	Exponential	-	IWC = aZ_e^b , a, b are constants	Z_e	EPM
CLOUDNET	Liquid part	-	-	LWC from LWP-scale with adiabatic gradient	T, P; LWP	Forward
	Ice part	-	spherical aggregates	IWC=F(Z_e, T)	T, P; Z_e	EPM
DENG	Ice	Exponential	hexagonal	Z_e=F(λ, N_0); V_d=F(λ, W_m); σ_d=F(λ, W_σ); W_σ=F(σ_d, Z_e);	Z_e, V_d, σ_d	Optimal
SHUPE_ TURNER	Pure liquid clouds	Log-normal	Spherical	r_e=F(Z, N) with adjusted N; LWC=F(Z)	Z, LWP	Forward
	Liquid & ice in optical thin clouds	Gamma	Any	Liquid and ice re: AERI based LWC: adiabatic gradient scaled by LWP; IWC=aZ_e^b	I; LWP	Optimal
	Ice in other clouds	exponential	-	IWC=aZ_e^b; r_e=F(Z_e); a=a(time), b=0.63	Z_e	EPM
WANG	Mixed	Modified gamma; log-normal	hexagonal	Ice part: IWC=F(σ_{ext}, r_e); r_e=F(σ_{ext}, Z_e); Liquid part: DISORT;	LWP, I, Z_e, σ_{ext}, T_{cb}	Forward Optimal
COMBRET	Liquid (radar)	Same as MICROBASE, except N=100 cm^{-3}				
	Ice (Z_e & σ_{ext})	Modified Gamma	hexagonal	IWC=F(σ_{ext}, Z_e); r_e=F(σ_{ext}, Z_e);	Z_e, σ_{ext}	EPM
	Ice (Z_e or σ_{ext})	Fitting Gamma	-	IWC=F(Z_e, T); IWC=F(σ_{ext}, T); r_e=F(IWC, Z_e); r_e=F(IWC, σ_{ext})	Z_e, T or σ_{ext}, T	EPM
	Drizzle and Rain	Marshall-Palmer type	-	R=F(Z); N(r)=F(R, r); r_e=volume/area;	Z	EPM
RADON	Ice	Normalized (N_0^*, D_m)	retrieved	ρ_I, V_t and w =f(V_d-Z relationship); IWC=f(Z_e, N_0^*), σ_{ext}=f(Z, N_0^*), D_m=f(V_T), r_e=F(IWC, σ_{ext});	Z_e, V_d	Forward
VARCLOUD	Ice	Normalized (N_0^*, D_m)	spherical aggregates	Radar and lidar forward models. (IR forward model available)	Z_e, σ_{ext}, I, T	Optimal

1210